

1 **Future projections of daily ~~hazy~~haze conducive and clear weather conditions over the**  
2 **North China Plain using a Perturbed Parameter Ensemble**

3 Shipra Jain<sup>1</sup>, Ruth M. Doherty<sup>1</sup>, David Sexton<sup>2</sup>, Steven Turnock<sup>2,3</sup>, Chaofan Li<sup>4</sup>, Zixuan Jia<sup>1</sup>,  
4 Zongbo Shi<sup>5</sup>, Lin Pei<sup>6</sup>

5 <sup>1</sup>School of GeoSciences, The University of Edinburgh, Edinburgh, United Kingdom

6 <sup>2</sup>Met Office Hadley Centre, Exeter, United Kingdom

7 <sup>3</sup>University of Leeds Met Office Strategic (LUMOS) Research Group, School of Earth and  
8 Environment, University of Leeds, UK

9 <sup>4</sup>Center for Monsoon System Research, Institute of Atmospheric Physics, Chinese Academy of  
10 Sciences, China

11 <sup>5</sup>School of Geography, Earth and Environmental Sciences, University of Birmingham,  
12 Birmingham, United Kingdom

13 <sup>6</sup>Institute of Urban Meteorology, China Meteorological Administration, Beijing, China

14  
15 **Corresponding Author:** Shipra Jain ([Shipra.Jain@ed.ac.uk](mailto:Shipra.Jain@ed.ac.uk))

## 16 Abstract

17 We examine past and future changes in both winter haze and clear weather conditions over the  
18 North China Plain (NCP) using a Perturbed Parameter Ensemble (PPE) and elucidate the  
19 influence of model physical parameterizations on these future projections for the first time. We  
20 use a large-scale meteorology-based Haze Weather Index (HWI), ~~which was developed to~~  
21 ~~examine the~~) with values  $>1$  as a proxy for haze conducive weather and HWI  $<-1$  for clear  
22 weather conditions ~~for Beijing. We find that the HWI can be used as an indicator of winter~~  
23 ~~haze across the entire over the~~ NCP ~~due to the extended spatial coherence of the local~~  
24 ~~meteorological conditions~~. The PPE generated using the UK Met Office HadGEM-GC3 model  
25 shows that under a high-emission (RCP8.5) scenario, the frequency of haze conducive weather  
26 (HWI $>1$ ) is likely to increase whereas the frequency of clear weather (HWI $<-1$ ) is likely to  
27 decrease in future. However, a change of opposite sign with lower magnitude in the  
28 frequencies, though less likely, is also possible. In future, the ~~total number of hazy~~  
29 daysfrequency of haze conducive weather for a given winter can be as much as  $\sim 3.5$  times  
30 higher than the numberfrequency of clear daysweather over the NCP. ~~We also examined the~~  
31 ~~changes in the interannual variability of the frequency of hazy and clear days and find no~~  
32 ~~marked changes in the variability for future periods.~~ The future frequencies of haze conducive  
33 weather (HWI $>1$ ) during winter ~~hazy and clear days in the PPE~~ are largely driven byassociated  
34 with changes in zonal-mean mid-tropospheric winds and the vertical temperature gradient over  
35 the NCP. We ~~do not also examined the changes in the interannual variability of the haze~~  
36 conductive and clear weather, and find ~~any discernible~~ no marked changes in the variability of  
37 future periods. We find a clear influence of model physical parametrizations on climatological  
38 mean frequencies for both haze conducive and clear weather. For mid to late 21<sup>st</sup> century (2033-  
39 2086), parametric effect can explain up to  $\sim 80\%$  variance in climatological mean frequencies  
40 of PPE members. Therefore, model parameterizations ~~on~~ adds uncertainty in the future

41 projections of ~~trends~~haze conducive weather in ~~addition to~~ the frequency of hazy or clear  
42 ~~days~~.internal variability. We also find a ~~clear impact~~growing influence of anthropogenic  
43 climate change on future ~~trends for both hazy and clear days, however, it is only discernible~~  
44 ~~for specific periods due to the large underlying internal variability in the frequencies of~~  
45 ~~hazy~~mean frequencies of haze conducive and clear days.

46 [weather over the 21<sup>st</sup> century suggesting climate change can exacerbate the haze conducive](#)  
47 [weather and reduce the clear weather conditions in future over the NCP.](#)

48

## 49 **1. Introduction**

50 Over the last decade, a number of severe haze episodes (several days or longer) were  
51 reported over the North China Plain (NCP) during boreal winter (December-January-February,  
52 DJF). In January 2013, unprecedented PM<sub>2.5</sub> levels exceeding 450 µg m<sup>-3</sup> were observed over  
53 the NCP (Wang et al., 2014a; Wang et al., 2014b; Zhang et al., 2018; Zhang et al., 2013).  
54 Similar events were also observed in November-December 2015 when the PM<sub>2.5</sub> concentrations  
55 reached as high as 1000 µg m<sup>-3</sup> in Beijing and caused the first-ever ‘red alert’ for severe air  
56 pollution (Liu et al., 2017; Zhang et al., 2017). In December 2016, around 25% of the land area  
57 of China was covered with severe haze for around one week (Yin and Wang, 2017). These  
58 severe haze events adversely impacted public health including mortality, visibility, and  
59 ultimately the economy of the country (Bai et al., 2007; Chen and Wang, 2015; Kan et al.,  
60 2012; Kan et al., 2007; Wang et al., 2006; Xu et al., 2013; Hong et al., 2019).

61 Previous research has shown that the persistence of severe haze for days during winters  
62 over the NCP occurred due to the combined effect of local and regional high pollutant  
63 emissions and stagnant meteorological conditions (Li et al., 2018; He et al., 2016; Jia et al.,  
64 2015; Pei et al., 2018; Zhang et al., 2021). The normal winter meteorological conditions over  
65 the NCP are characterized by northwesterly flow near the surface through to the mid-  
66 troposphere associated with the East Asian winter monsoon ([circulation \(Fig. 1a and 1b; also](#)  
67 [see An et al., 2019; Chen and Wang, 2015; Li et al., 2016; Renhe et al., 2014; Li et al., 2016;](#)  
68 [Xu et al., 2006\).](#) [The northwesterly winds support the intrusion of relatively clean air from the](#)  
69 [high latitudes to the NCP and therefore ventilate this region \(Xu et al., 2006\).](#) However, during

70 the severe haze episodes, the near-surface northwesterlies appear to be weaker than normal and  
71 the mid-tropospheric trough was reported to be shallower and shifted northwards – collectively  
72 leading to a weaker than normal northwesterly flow and reduced horizontal transport of air  
73 pollutants from the NCP (Chen and Wang, 2015). The weaker northwesterlies near the surface  
74 also reduces the intrusion of cold and clean air from the high latitudes to the NCP (Xu et al.,  
75 2006); Fig. 2a-b). In addition to changes in horizontal winds, the vertical temperature gradient  
76 between the lower and upper troposphere over the NCP enhance can influence the vertical  
77 dispersion of the pollutants. A warmer than normal temperature near the surface, accompanied  
78 with colder temperature in the upper troposphere, would enhance the thermal stability and  
79 reduces reduce the atmospheric mixing leading to the build-up of the atmospheric pollutants  
80 over this region (Fig. 2; also see Hou and Wu, 2016; Sun et al., 2014; Wang et al., 2014a;  
81 Zhang et al., 2018; Cai et al., 2018). The planetary boundary layer height is also found to be  
82 suppressed during extreme haze events leading to accumulation of pollutants, notably PM<sub>2.5</sub>  
83 concentrations (Liu et al., 2018; Petäjä et al., 2016), due to an increase in moisture, reduced  
84 vertical mixing and dispersion which aids aerosol growth during high haze events over the  
85 NCP (An et al., 2019; Tie et al., 2017).

86 ~~In this paper, our focus is on~~ On a daily scale, past studies have examined the  
87 ~~meteorological driven changes leading to daily hazy or clear in haze conducive~~ weather  
88 conditions over ~~the NCP. On a daily scale, recent studies suggest an increase in the occurrence~~  
89 ~~of large-scale meteorological conditions favourable for winter haze over the NCP~~ China under  
90 climate change: scenarios using large-scale meteorology-based indexes. For example, Cai et  
91 al. (2017) have used four key variables, i.e. meridional wind at 850 hPa ( $V_{850}$ ), zonal wind at  
92 500 hPa ( $U_{500}$ ), temperatures at 850 hPa ( $T_{850}$ ) and 250 hPa ( $T_{250}$ ) pressure levels to calculate  
93 a meteorology-based daily Haze Weather Index (HWI) ~~and~~. They have projected a ~50%  
94 increase in the frequency of winter haze conducive weather conditions, similar to the January

95 2013 event, over Beijing in the future (2050-2099) as compared to the historical (1950-1999)  
96 period under [the RCP8.5 scenario using 15 CMIP5 models](#). Using the HWI, Liu et al. (2019)  
97 [projected a 6-9% increase in the winter haze frequency under 1.5° and 2° global warming,](#)  
98 [respectively based on 20 CMIP5 models whereas Qiu et al. \(2020\) projected a relatively high](#)  
99 [increase of 21% and 18% in severe winter haze episodes under 1.5° and 2° global warming,](#)  
100 [respectively using an ensemble of climate simulations from the Community Earth System](#)  
101 [Model 1 \(CESM1\) \(Kay et al., 2015\).](#) ~~RCP8.5 scenario using 15 CMIP5 models.~~ Han et al.  
102 (2017) ~~also~~ Callahan and Mankin (2020) also used specific humidity,  $V_{850}$ ,  $T_{850}$  and  
103 [temperatures at 1000 hPa to examine the haze favourable meteorology for Beijing, and found](#)  
104 [a 10-15% increase in winter haze conducive weather in CMIP5 multimodel and CESM large](#)  
105 [ensemble under 3° warming. These authors have also emphasized a large influence of internal](#)  
106 [variability in addition to anthropogenic forcing on future haze conducive weather over Beijing.](#)

107 [In addition to the large-scale meteorology based indexes, several other stagnation](#)  
108 [indices based on regional or local meteorological variables have also been used to determine](#)  
109 [the influence of anthropogenic climate change on haze conducive weather for China as well as](#)  
110 [global regions. Using minimum monthly mean wind speeds averaged over northwestern](#)  
111 [Europe, Vautard et al. \(2018\) suggested a potential increase in the frequency of stagnant](#)  
112 [conditions conducive to air pollution over northwest Europe; however, their results were](#)  
113 [sensitive to models used for the analysis. Horton et al. \(2014\) have used thresholds for the daily](#)  
114 [mean near-surface \(10-m\) wind speeds, mid-tropospheric \(500 hPa\) temperatures and](#)  
115 [accumulated precipitation to calculate the Air Stagnation Index \(ASI\) under RCP8.5 scenario](#)  
116 [using 15 CMIP5 models. They found an increase in air stagnation occurrence events leading to](#)  
117 [poor air quality by up to ~40 days per year over a majority of the tropics and sub-tropics. Han](#)  
118 [et al. \(2017\) examined indicators of haze pollution potential \(e.g. horizontal transport, wet-](#)  
119 [deposition, ventilation conditions\) using three regional climate simulations and projected a](#)

120 higher probability of haze pollution risk over [the](#) Beijing-Tianjin-Hebei region under the  
121 RCP4.5 scenario. [LiuGarrido-Perez et al. \(2019\)](#) projected(2021) took a 6-9% increase in the  
122 [winter haze frequency under 1.5°](#) different approach as compared to analysing probabilistic  
123 [projections](#) and 2° global warming, respectively used the ASI to generate stagnation storylines,  
124 [i.e. plausible and physically consistent scenarios of stagnation changes](#) based on 20 CMIP5  
125 [models](#). [Qiu et al. \(2020\)](#) also projected an increase of 21% and 18% in severe winter haze  
126 [episodes under 1.5° and 2° global warming, respectively using an ensemble](#) the response of  
127 [remote drivers under climate simulations from the Community Earth System Model 1](#)  
128 [\(CESM1\) for a low warming experiment change](#)([Kay et al., 2015](#)). [Callahan and Mankin](#)  
129 [\(2020\)](#) found 10-15% increase in winter hazy days in CMIP5 multimodel and CESM large  
130 [ensemble under 3° warming and emphasized a large influence of internal variability in addition](#)  
131 [to anthropogenic forcing on future, for Europe and the United States \(US\)](#).

132 [While most studies indicate an increase in the](#) haze conducive weather over [Beijing](#).  
133 [AChina, a](#) few studies also find little impact of climate change on future projections of haze  
134 (Shen et al., 2018; Pendergrass et al., 2019), which could partly arise due to the under-sampling  
135 of internal variability associated uncertainty in their projections (Callahan and Mankin, 2020),  
136 as well as model-to-model differences. Hence, there is a large uncertainty as to how haze  
137 conducive weather conditions may change in the future and these depend on haze [metrics](#)  
138 or underlying processes considered for [future](#) projections.

139 In order to account for the uncertainty in the future projections (e.g. of large-scale  
140 circulation) particularly at the regional scale (Hawkins and Sutton, 2012; Deser et al., 2012;  
141 Deser et al., 2014), it is desirable to use an ensemble of climate change simulations. Whilst a  
142 multimodel ensemble, e.g. CMIP5 or CMIP6, is commonly used for climate change studies,  
143 several other studies have also emphasised the use of an initialised ensemble or Perturbed  
144 Parameter Ensemble (PPE) from a single model to assess the uncertainties and obtain a

145 comprehensive range of possible future climate realisations for the same emission scenario for  
146 a given model (Knutti et al., 2010). All three methodologies have different advantages. For  
147 instance, using multiple models allows us to sample structural uncertainty in future projections,  
148 which cannot be sampled using a single model. On the other hand, using an initialised ensemble  
149 from a single model allows us to sample a broader range of internal variability, which is often  
150 under-sampled in a multimodel ensemble. The advantage of using the PPE over the initialised  
151 or multimodel ensemble is that it not only accounts for internal variability but also model  
152 uncertainty arising due to the different settings of the physical parameterisations in a single  
153 model.

154 ——— Both multimodel ensemble and initialised ensemble from a single model have been  
155 used to assess the future winter haze conducive conditions over Beijing. In this paper, we use  
156 a PPE generated using the UK’s Met Office HadGEM-GC3 model to assess for the first time  
157 the impact of both model physical parameterisations and anthropogenic climate change on  
158 future daily haze conducive weather conditions ~~using the HWI. We first determine the spatial~~  
159 ~~extent for which the HWI can be used as an indicator of air quality over China (Section 3). We~~  
160 ~~examine the changes in the frequency of hazy and clear days for historical and three future~~  
161 ~~periods, i.e. near (2006–2032), mid (2033–2059) and far (2060–2086) future, over the NCP~~  
162 ~~(Section 4). We also analyse the changes in the interannual variance of the frequency of hazy~~  
163 ~~and clear days for the future periods as compared to the historical (Section 5). We investigate~~  
164 ~~the importance of the different meteorological variables used in the HWI in determining the~~  
165 ~~future changes in haze conducive conditions in the PPE (Section 6). Finally, we assess the~~  
166 ~~model physical parameterisations and anthropogenic climate change on the frequency of future~~  
167 ~~hazy and clear weather conditions over the NCP (Section 7). More details on the data and~~  
168 ~~methods used in this paper are provided in the next section.~~

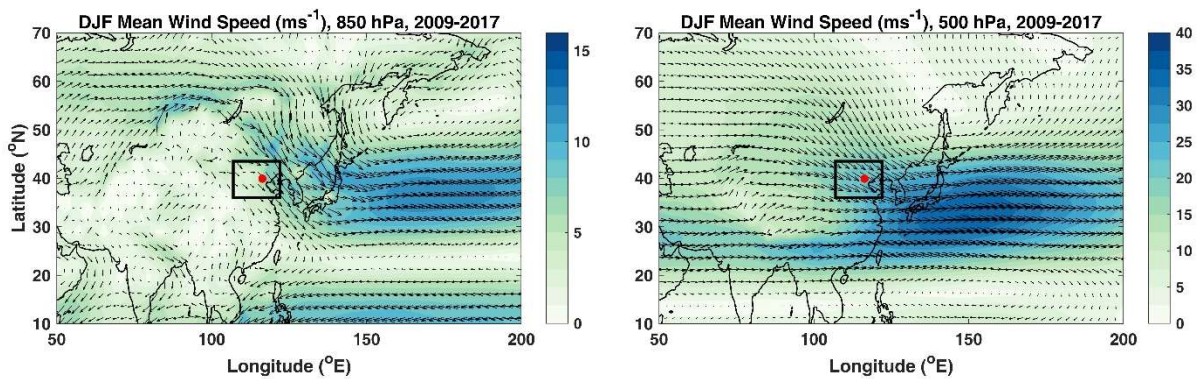


169 In this paper, our focus is on the daily haze conducive and clear weather conditions  
170 over the NCP under a fixed high-emission scenario (RCP8.5). For this purpose, we use the  
171 HWI proposed by Cai et al. (2018) as past research studies have shown a robust correlation  
172 between the HWI, which is a large-scale meteorology based index, and haze conducive weather  
173 for Beijing in China. Whilst Cai et al. (2018) originally proposed the HWI for Beijing, the  
174 index is based on changes in large-scale meteorology over the NCP and thus offers a good  
175 potential as the indicator of haze conducive weather over the NCP. One potential advantage of  
176 using the HWI for future projections, as opposed to a regional or local air stagnation index, is  
177 that the general circulation models generally simulate large-scale meteorology reasonably well  
178 as compared to local or regional meteorology. Therefore, we expect the future projections of  
179 clear or haze conducive weather provided using the HWI to be less uncertain than projections  
180 provided using regional stagnation indexes.

181 The HWI uses four meteorological variables as stated above, but Cai et al. (2018) have  
182 also examined the impact of the inclusion of more weather variables, such as geopotential  
183 height, boundary layer thickness and local stratification instability, in the HWI and did not find  
184 any significant differences in the performance of the HWI. Therefore, we use the same  
185 variables and methodology as Cai et al (2018) to calculate the HWI and provide future  
186 projections of haze conducive and clear weather using the HWI. However, our analysis is based  
187 on an underlying assumption that the large-scale meteorological conditions, which are used as  
188 a basis for the HWI, will have a similar influence on the air quality of the NCP in the future  
189 climate as for present-day climate.

190 In this paper, we first examine the application of the HWI as a proxy for haze conducive  
191 and clear weather over NCP for the current climate using a suite of observations (Section 3).  
192 We then provide the projections of the haze conducive (HWI >1) and clear weather (HWI <-  
193 1) frequency over NCP for the historical and future period. We assess the impact of model

194 [physical parametrisations and anthropogenic climate change on the frequencies \(Section 4\).](#)  
195 [We also analyse the changes in the interannual variance of the frequency of haze conducive](#)  
196 [and clear weather conditions for the future periods as compared to the historical period \(Section](#)  
197 [5\). Finally, we assess the impact of parametric effect and anthropogenic climate change on](#)  
198 [trends in haze conducive and clear weather occurrence over the 21<sup>st</sup> century \(Section 6\). Details](#)  
199 [of data and methods used in this paper are provided in the next section.](#)



201 [Figure 1 Average wind speed at \(a\) 850 hPa and \(b\) 500 hPa pressure level. The red dot](#)  
202 [represents the location of Beijing and black rectangle shows the location of the NCP. This](#)  
203 [figure has been repeated for a longer average period, i.e. 1979-2019 \(not shown\) and the result](#)  
204 [is similar.](#)

## 205 **2. Data & Methods**

### 206 **2.1 Observations, Reanalysis Outputs and PPE Model Simulations**

207 Hourly PM<sub>2.5</sub> concentrations are used from the US embassy site for Beijing for DJF  
208 from 2009-2017. Daily mean PM<sub>2.5</sub> concentrations are constructed using hourly data to [identify](#)  
209 [hazy and clear days and](#) evaluate the performance of the HWI [as a representative of haze](#)  
210 [conductive and clear weather conditions](#) for Beijing (see Section 3). We also used newly  
211 released gridded daily PM<sub>2.5</sub> concentrations for DJF from Chinese Air Quality Reanalysis  
212 Datasets (CAQRA) provided by China National Environment Monitoring Centre for 2013-  
213 2017 (Kong et al., 2021) to test the performance of the HWI across entire China. The CAQRA  
214 data has been produced by assimilating surface air quality observations from over 1000

215 monitoring sites in China and is available at a high spatial resolution of around 15×15 km and  
216 hourly temporal resolution over China. More details on the validation of the CAQRA dataset  
217 against the independent station data is provided in (Kong et al., (2021)). The visibility data for  
218 Beijing (homogenized data for 20 stations in Beijing) is provided by the National  
219 Meteorological Information Center of China, [ChineseChina](#) Meteorological  
220 [AgencyAdministration \(CMA\)](#), for DJF 1999-2018.

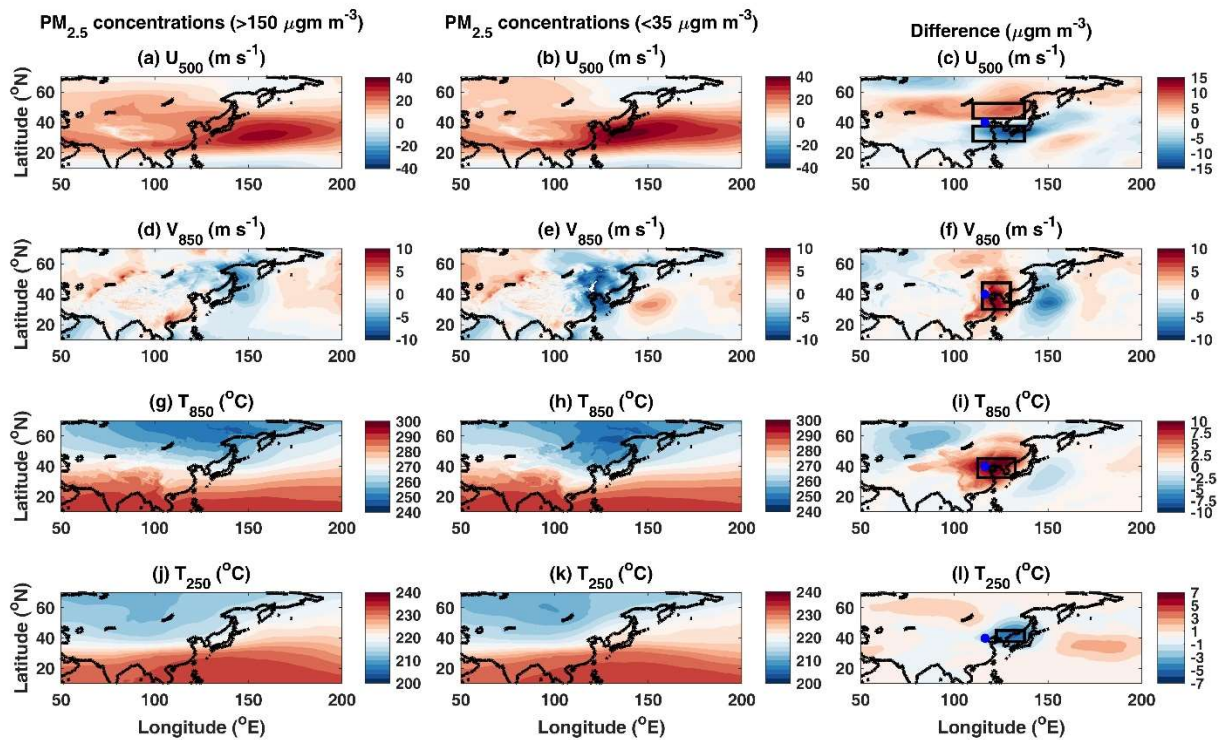
221 We used daily ERA-5 reanalysis data of four variables: meridional wind at 850 hPa  
222 pressure level ( $V_{850}$ ), zonal wind at 500 hPa pressure level ( $U_{500}$ ), temperatures at 850 hPa  
223 level ( $T_{850}$ ) and 250 hPa ( $T_{250}$ ) to calculate the HWI for DJF 1979-2019. The ERA-5 data used  
224 here is available at 0.25° x 0.25° horizontal resolution and hourly temporal resolution  
225 (Hersbach et al., 2020).

226 We used a PPE of climate simulations produced using the recent configuration of the  
227 UK Met Office's HadGEM3-GC3.05 coupled model (Sexton et al., 2021; Yamazaki et al.,  
228 2021). The base model used for PPE, HadGEM3-GC3.05, has a horizontal resolution of ~60  
229 km with 85 vertical levels. A total of 47 model parameters from seven parameterization  
230 schemes were simultaneously perturbed to obtain the PPE (the full list of perturbed parameters  
231 is provided in Table 1 of (Sexton et al., 2021). Here, we used daily outputs of  $V_{850}$ ,  $U_{500}$ ,  $T_{850}$   
232 and  $T_{250}$  for DJF for the historical (1969-2005) and future (2006-2089) under the RCP8.5  
233 scenario. In addition, we also assessed internal variability using 200-year control simulations  
234 for each PPE member where 1900 boundary conditions were prescribed. Overall, 16 PPE  
235 members are available for all the control, historical and RCP8.5 simulations.

## 236 **2.2 Calculation of the HWI**

237 The winter HWI is calculated using the methodology given by Cai et al. (2017). We  
238 analyse the composite differences in the  $U_{500}$ ,  $V_{850}$ ,  $T_{850}$  and  $T_{250}$  for hazy ( $PM_{2.5}$  concentrations

239  $> 150 \mu\text{g m}^{-3}$  [for Beijing](#)) and clear ( $\text{PM}_{2.5}$  concentrations  $< 35 \mu\text{g m}^{-3}$  [for Beijing](#)) days across  
 240 China for DJF 2009-2017 (Fig. 42) (see [next](#) section 3.1 for [an explanation on the  \$\text{PM}\_{2.5}\$](#)   
 241 [concentration](#) cut-offs values used [for  \$\text{PM}\_{2.5}\$  concentration](#)). [here](#)). We also provide the  
 242 [composite values for these meteorological variables for hazy and clear days separately in Fig.](#)  
 243 [2.](#)



244  
 245 **Figure 4** shows the 2 Winter composites of u-wind at 500 hPa level ( $U_{500}$ ) over China for all  
 246 [available days for which data is available from US embassy station for Beijing for DJF 2009-](#)  
 247 [2017 for \(a\) high  \$\text{PM}\_{2.5}\$  \( \$>150 \mu\text{g m}^{-3}\$ \), \(b\) low  \$\text{PM}\_{2.5}\$  \( \$<35 \mu\text{g m}^{-3}\$ \) concentrations and \(c\)](#)  
 248 [difference in the zonal wind speed with a dipole pattern suggesting a northward shift in between](#)  
 249 [the composites in \(a\) and \(b\). \(d-f\) same as \(a-c\) but for v-wind at 850 hPa level \( \$V\_{850}\$ \), \(g-i\)](#)  
 250 [same as \(a-c\) but for temperature at 850 hPa level \( \$T\_{850}\$ \), and \(j-l\) same as \(a-c\) but for](#)  
 251 [temperature at 250 hPa pressure level \( \$T\_{250}\$ \). Black rectangles \(B1-B5\) in the last column show](#)  
 252 [the regions for which spatial means were used for the calculation of the HWI. The blue dot in](#)  
 253 [these columns shows the location of Beijing.](#)

254 [During the hazy days, the mid-tropospheric trough \(Fig. 1a\), weakened westerly flow](#)  
 255 [becomes weaker over the NCP as compared to the clear days \(Fig. 2a-c\). The mid-tropospheric](#)  
 256 [trough also moves northwards as suggested by the dipole pattern in Fig 2c, which shows the](#)  
 257 [differences in the  \$U\_{500}\$  for hazy and clear days. The northerly flow \(Fig. 1b\), higher](#)  
 258 [temperatures in the near the surface is weaker during hazy days as compared to clear days \(Fig.](#)

259 2d-f). The lower troposphere and lower temperatures in is relatively warmer during hazy days  
260 as compared to clear days (Fig. 2g-i) whereas the upper troposphere (Fig. 1e-d) is cooler over  
261 the NCP during hazy days as compared to the clear days. These findings (Fig. 2j-l). The changes  
262 in these variables are also consistent with the previous studies (e.g. Cai et al., 2017) that showed  
263 similar changes in these meteorological variables. Cai et al. (2018) have examined the use of  
264 other variables such as geopotential height, boundary layer thickness and local stratification  
265 instability and do not find any significant differences in the performance of HWI by inclusion  
266 of more weather parameters for this time period. Therefore, we also use only these four  
267 variables for our analysis the calculation of the HWI, which is used as a proxy for haze  
268 conducive and clear weather conditions under a future climate.

269 ~~The winter HWI is calculated using the methodology given by Cai et al. (2017).~~ For the  
270 calculation of observational HWI, we use ERA-5 reanalysis data for the period 1979-2019. We  
271 first create a daily DJF time series of each variable for each reanalyses grid point over China.  
272 The daily DJF time series is concatenated for the period 1979-2019. A daily standardised  
273 anomaly time series is created for each meteorological variable by first removing the daily  
274 mean climatology from each day of the time series and then normalising by the standard  
275 deviation. Spatial averages are then obtained over the relevant boxes (B1 to B5) for each  
276 meteorological variable following Cai et al. (2017) (Fig. 1). The HWI time-series is calculated  
277 by using the following equation:

$$278 \quad \text{HWI}(t) = U_{500}(t) + V_{850}(t) + dT(t)$$

279 where  $U_{500} = U_{500,B1}(t) - U_{500,B2}(t)$ ,  $V_{850} = V_{850,B3}(t)$ , and  $dT = T_{850,B4}(t) - T_{250,B5}(t)$ . The HWI  
280 (t) time series is then itself normalized by its own standard deviation.

281 For the PPE historical and RCP8.5 simulations, the daily HWI time series is calculated  
282 for each ensemble member for DJF for 1969-2089 using the same methodology as used for



283 ERA-5, with the difference being that the normalisation of the PPE time-series (1969-2089) is  
284 performed using the historical standard deviation (1969-2005), following Cai et al. (2017).  
285 Similarly, the HWI time series is calculated for the PPE pre-industrial control simulations for  
286 170 model years out of 200 model years (the first 30 years are discarded as model spin-up  
287 period). The normalisation of the pre-industrial control time series is performed using the  
288 standard deviation for 170 years. The pre-industrial control simulations used here are initialised  
289 with past forcings corresponding to the year 1900 and therefore are an approximate  
290 representative representation of the internal variability of the current climate as this does not  
291 take into account any temporal changes in the internal variability from 1900 to the historical  
292 and future periods used here.

### 293 **3. Relationship between the Haze Weather Index as an indicator for clear and air quality** 294 **indicators haze conducive weather conditions over the NCP**

295 We determine As the relationship between HWI and PM<sub>2.5</sub> concentration was originally  
296 proposed for Beijing. As visibility is an optical by Cai et al. (2018), we first determine if the  
297 HWI can be used as a representative of haze (Wang et al., 2006) conductive and available clear  
298 weather conditions for a relatively long period (1999–2018) as compared to the present climate  
299 for Beijing using (a) PM<sub>2.5</sub> concentrations, we also correlate the HWI with from the visibility  
300 over US embassy station in Beijing. We then test the relationship between HWI and (b) PM<sub>2.5</sub>  
301 concentrations over entire China to averaged over larger Beijing domain from CAQRA  
302 reanalysis and (c) visibility data from the CMA stations in Beijing. We then determine the  
303 spatial extent of the region for which HWI can be used as an indicator of air quality haze  
304 conductive and clear weather conditions using PM<sub>2.5</sub> concentrations for China using CAQRA  
305 reanalysis data. We use the 25<sup>th</sup> and 75<sup>th</sup> percentile values of daily mean PM<sub>2.5</sub> concentrations  
306 to identify the clear and hazy days, respectively for each dataset. For visibility, we use the  
307 opposite criterion, i.e. 25<sup>th</sup> percentile as a threshold for hazy days and 75<sup>th</sup> percentile as a

308 threshold of clear days, as lower visibility is associated with hazy days and higher visibility  
309 with clear days. The days with daily PM<sub>2.5</sub> concentration or visibility lying between the 25<sup>th</sup>  
310 and 75<sup>th</sup> percentile values are identified as moderately polluted days.

### 311 3.1 PM<sub>2.5</sub> concentrations for Beijing versus HWI

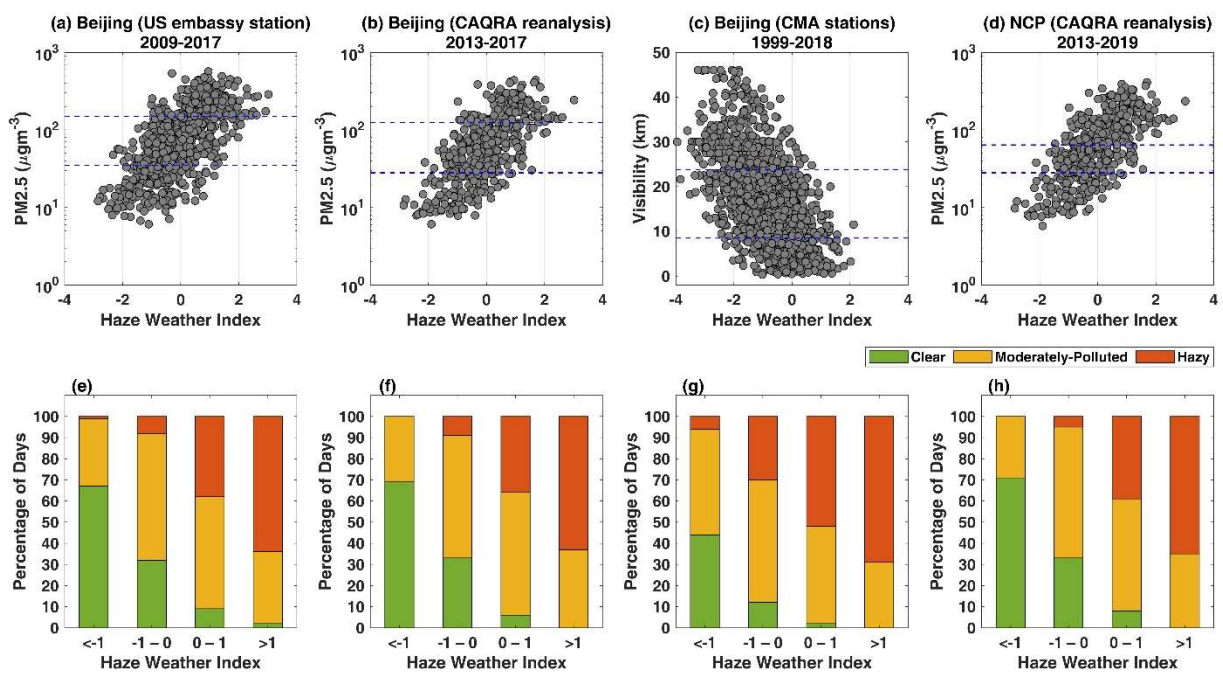
312 Figure 2 We examine the relationship between the daily HWI and PM<sub>2.5</sub>  
313 concentrations for the US embassy station for Beijing. Figure 3 (a) shows that the daily HWI  
314 increases linearly with increasing PM<sub>2.5</sub> concentrations for up to ~150 µg m<sup>-3</sup> and ~~for~~ PM<sub>2.5</sub> >  
315 150 µg m<sup>-3</sup>, the HWI starts to level-off (note the log scaling in the y-axis). The time-series  
316 correlation between the HWI and PM<sub>2.5</sub> concentration is ~0.58, which is significant at the 1%  
317 level. Callahan et al. (2019) have also obtained a correlation coefficient of 0.58 for daily PM<sub>2.5</sub>  
318 concentrations from the U.S. embassy in Beijing and the HWI calculated using NCAR R1  
319 reanalysis.

320 The 25<sup>th</sup> and 75<sup>th</sup> percentile values of daily mean PM<sub>2.5</sub> concentrations for the US  
321 embassy Beijing station for DJF 2009-2017 are ~35 and ~150 µg m<sup>-3</sup> respectively. We  
322 determine the percentage of hazy days (with daily mean PM<sub>2.5</sub> concentrations >150 µg m<sup>-3</sup>) and  
323 clear days (with daily mean PM<sub>2.5</sub> concentrations < 35 µg m<sup>-3</sup>) for different HWI ranges (Fig.  
324 2b3e). Out of all days with HWI >1, 64% have daily mean PM<sub>2.5</sub> concentrations > 150 µg m<sup>-3</sup>  
325 and 98% with PM<sub>2.5</sub> concentrations >35 µg m<sup>-3</sup>. This suggests that for HWI >1, almost all days  
326 are hazy or moderately polluted. Similarly, almost all days with HWI < -1 are clear or  
327 moderately polluted. Using HWI thresholds of ±1 demarcates between the clear and hazy days,  
328 i.e. almost no clear days occur for HWI >1 and almost no hazy days occur for HWI <-1.

329 We have also examined the relationship between the individual variables in the HWI  
330 (section 2.2) and PM<sub>2.5</sub> concentrations observed at the US embassy in Beijing/CAQRA and  
331 find that the individual components have correlation values that are similar to or less than that

332 [of those used in the combined HWI. Also, physically multiple favourable weather conditions,](#)  
 333 [as represented by each of these variables, collectively provide a conducive setting for haze.](#)  
 334 [Hence, we focus on the HWI as a combined index rather than its individual components.](#)

335 [To examine if the PM<sub>2.5</sub> concentrations from the US embassy station are sensitive to](#)  
 336 [the abrupt changes in the local meteorology, e.g. wind speeds or direction, we also examine](#)  
 337 [the relationship between the HWI and PM<sub>2.5</sub> concentrations averaged over the domain centred](#)  
 338 [around Beijing \(116.15 – 116.65 °E, 39.65 – 40.15 °N\) from the CAQRA reanalysis data \(Fig.](#)  
 339 [3b and 3f\). The PM<sub>2.5</sub> concentrations for region spatially averaged around Beijing from](#)  
 340 [CAQRA data are in the range 6 μg m<sup>-3</sup> – 441 μg m<sup>-3</sup> and from the Beijing US embassy station](#)  
 341 [are 6 μg m<sup>-3</sup> – 569 μg m<sup>-3</sup> suggesting the values from both data sources are comparable. The](#)  
 342 [correlation coefficient is ~0.58, which is the same as the correlation obtained using the US](#)  
 343 [embassy data. The total number of hazy, clear and moderately polluted days for different HWI](#)  
 344 [ranges also show similar results for both datasets \(Fig. 3e-3f\). This implies that the HWI](#)  
 345 [relationship with PM<sub>2.5</sub> concentrations is robust across different data sources and that PM<sub>2.5</sub> is](#)  
 346 [a regional pollutant.](#)



347



348 [Figure 3](#) HWI versus daily mean (a)  $PM_{2.5}$  concentrations for the US embassy Beijing station for DJF  
349 2009-2017 (b)  $PM_{2.5}$  concentrations spatially averaged over the region around Beijing (116.15-116.65  
350 °E, 39.65 - 40.15 °N) from CAQRA reanalysis for DJF 2013-2017 (c) visibility averaged over 20  
351 stations from the CMA for DJF 1999-2018 and (d)  $PM_{2.5}$  concentrations spatially averaged over the  
352 NCP (36-43.5 °N, 107-122 °E) from CAQRA reanalysis. Blue lines show the 25<sup>th</sup> and 75<sup>th</sup> percentile  
353 thresholds used to define clear and hazy days for each dataset. Percentage of clear, moderately polluted  
354 and hazy days for different HWI ranges for the (e) US embassy Beijing station for DJF 1999-2018 (f)  
355 larger Beijing domain (116.15-116.65 °E, 39.65 - 40.15 °N) from CAQRA reanalysis for DJF 2013-  
356 2017 (g) Beijing for DJF 1999-2018 (h) NCP from the CAQRA reanalysis for DJF 2013-2017.

### 357 **3.2 Visibility for Beijing versus HWI**

358 [As visibility is an optical representative of haze \(Wang et al., 2006\) and the data for](#)  
359 [visibility is available for a relatively long period \(1999-2018\) as compared to the  \$PM\_{2.5}\$](#)   
360 [concentrations, we also correlate the HWI with the visibility over Beijing. ~~Figure 33-2~~](#)

### 361 **Visibility for Beijing versus HWI**

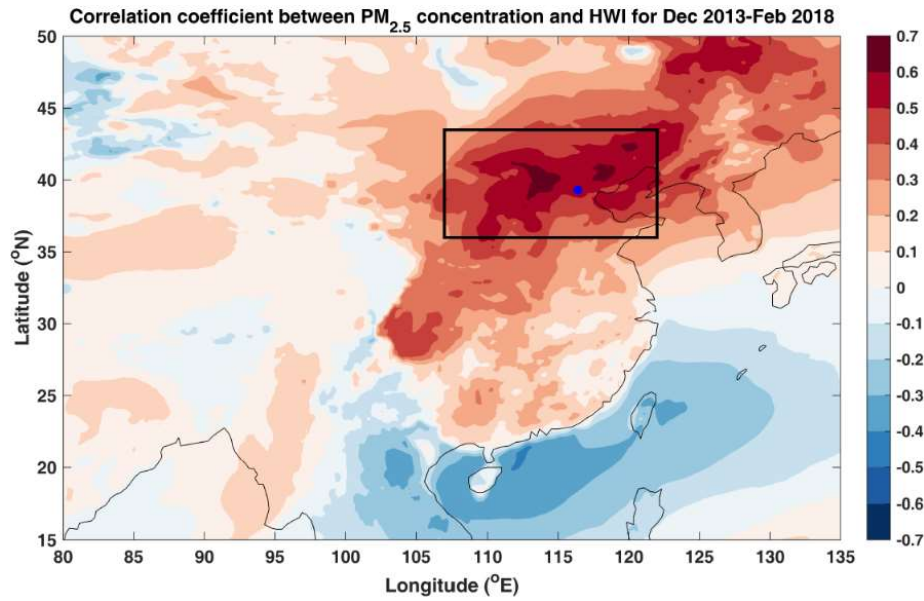
362 [Figure 2](#) (c) shows that the HWI is inversely related to the visibility for the Beijing  
363 station. The time-series correlation between the HWI and visibility is -0.63, which is significant  
364 at the 1% level. The days with visibility < 8.5 km are identified as hazy days, days with  
365 visibility > 23.8 km are identified as clear days. For days with HWI > 1, no clear days occur  
366 and similarly for days with HWI < -1, only 6% of days are hazy (Fig [243g](#)). This further  
367 confirms that the correlation between the HWI and haze is significant for a longer period (1999-  
368 2018) using visibility as a metric for haze (alternative to the  $PM_{2.5}$  concentrations used above).

### 369 **3.3 $PM_{2.5}$ concentrations over North China Plain versus HWI**

370 We now determine the spatial extent for which HWI can be used as an indicator of [haze](#)  
371 [clear or haze conducive conditions using](#)  $PM_{2.5}$  concentrations ~~using data~~ from CAQRA  
372 reanalysis. We correlate the daily time-series of  $PM_{2.5}$  concentration at each grid point with the  
373 HWI for DJF 2013-2017 (Fig. [34](#)). Over the entire NCP (36-43.5 °N, 107-122 °E), the  
374 correlation coefficient between the daily HWI and gridded  $PM_{2.5}$  concentration is ~0.7,  
375 significant at the 1% level. The correlation is considerably lower but still significant over other

376 eastern China regions, e.g. north easternmost China and the Sichuan Basin (27-32 °N, 102-107  
377 °E).

378



379

380 **Figure 34** Spatial distribution of correlation between winter PM<sub>2.5</sub> concentrations and HWI time series  
381 at each grid point. Blue dot shows the Beijing station (39.3 °N, 116.4 °E) and the black rectangle shows  
382 the North China Plain (36-43.5 °N, 107-122 °E).

383

384

385

386

387

388

389

390

391

392

393

394

Considering daily mean PM<sub>2.5</sub> concentrations averaged over the NCP, we also find a linear relationship with the daily HWI ( $r = 0.66$ ; significant at the 1% level; Fig 2e). ~~The values of PM<sub>2.5</sub> concentrations for NCP are lower as compared to the station values of PM<sub>2.5</sub> concentrations at the US Embassy Beijing and the correlation coefficient is higher. This could be due to the different time periods for the two dataset, i.e. 2009-2017 for the US embassy and 2013-2017 for the CAQRA reanalyses, and spatial averaging of PM<sub>2.5</sub> concentrations over the NCP region.2d).~~ We also calculate the percentage of clear and hazy days for different HWI ranges for the larger domain of the NCP using the 25<sup>th</sup> and 75<sup>th</sup> percentile values, respectively. The percentage of hazy and clear days for HWI > 1 and HWI < -1 for NCP in CAQRA reanalyses are very similar to the values obtained for the US embassy Beijing station (Fig 2f3h).

Overall, our results confirm that the daily HWI has a robust relationship with daily PM<sub>2.5</sub> concentrations not only for the Beijing station but across the NCP for the given time

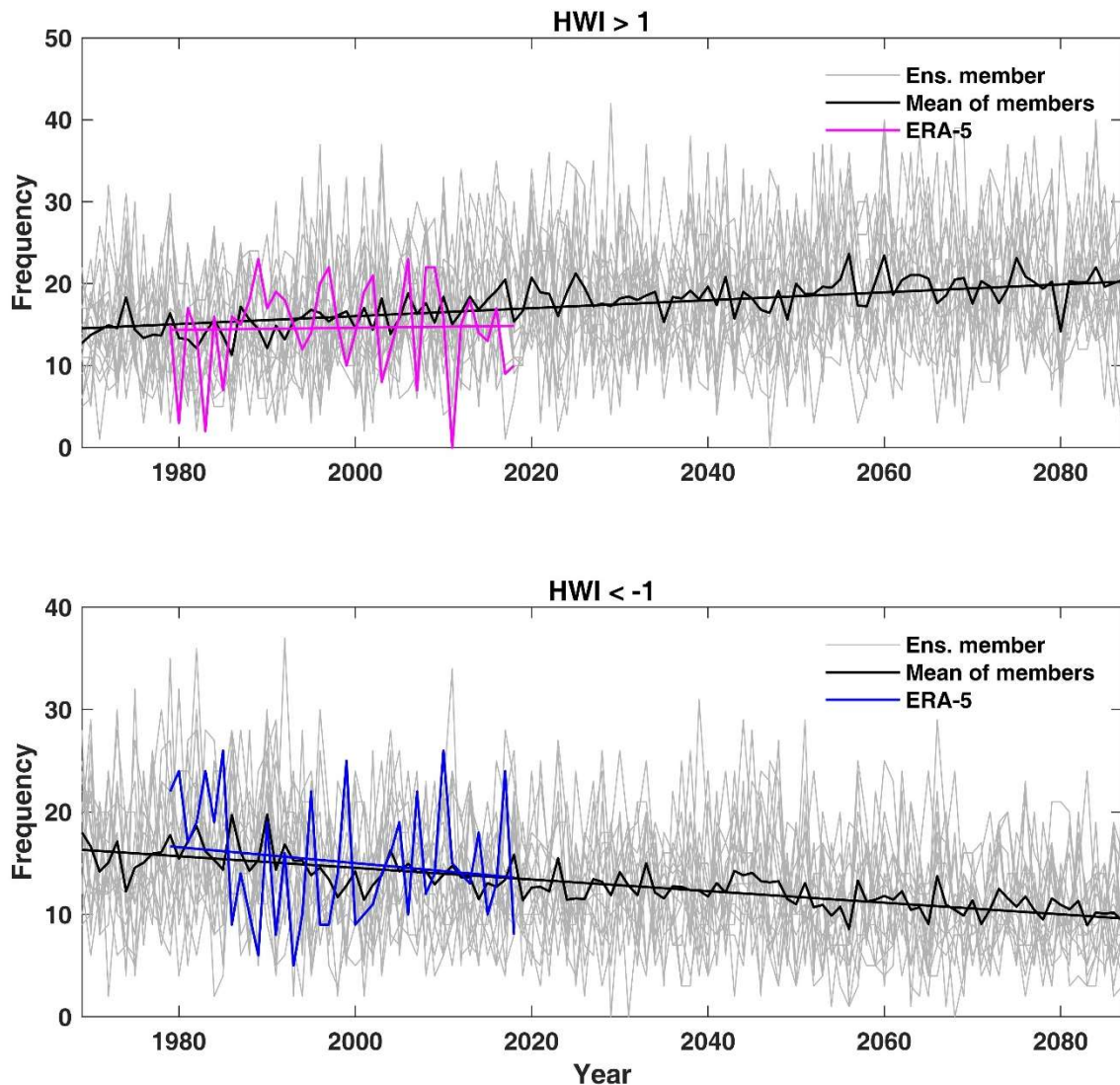
395 periods. Therefore, we use  $HWI > 1$  as a ~~threshold proxy~~ for ~~hazy days~~ haze conducive weather  
396 and  $HWI < -1$  as a ~~threshold of proxy for~~ clear days ~~weather~~ across the NCP region. This  
397 threshold is also consistent with several other studies (e.g., Cai et al., 2017; Callahan and  
398 Mankin, 2020; Callahan et al., 2019), that have used  $HWI > 1$ , as a cut-off for ~~hazy days~~ haze  
399 conductive weather for Beijing. We now ~~use the HWI to~~ calculate the frequency of hazy haze  
400 conductive weather ( $HWI > 1$ ) and clear ~~conditions~~ weather ( $HWI < -1$ ) for the past and future  
401 using ERA-5 reanalysis and PPE members.

#### 402 **4. Historical and future changes in ~~the frequency of hazy~~ haze conducive and clear** 403 **conditions weather occurrence**

404 The ~~changes in the number of hazy~~ frequency of haze conducive weather ( $HWI > 1$ ) and  
405 clear ~~days per winter, as defined by HWI thresholds,~~ weather ( $HWI < -1$ ) from the ERA-5  
406 reanalyses and the PPE are shown in Fig. 45. For ERA-5, the frequency of ~~hazy days~~ haze  
407 conductive weather has increased, whereas the frequency of clear days weather ( $HWI < -1$ ) has  
408 reduced for the period 1979-2018. The mean frequency of ~~hazy days~~ haze conducive weather  
409 using 16 PPE members shows a relatively larger increase than ERA-5 for the same 1979-2018  
410 time-period (Fig. 4a5a). In contrast, the mean frequency of clear days weather from the PPE  
411 for this period shows a similar reduction to that obtained using the ERA-5 reanalyses (Fig.  
412 4b5b).

413 We examine the changes in the frequency of hazy haze conducive weather ( $HWI > 1$ )  
414 and clear days weather ( $HWI < -1$ ) for the historical (1979-2005) and three future periods, i.e.  
415 near (2006-2032), mid (2033-2059) and far (2060-2086) future. The mean frequency ~~of hazy~~  
416 days for haze conducive weather is 14.7 days per winter obtained from the ERA-5 reanalysis  
417 and 15.0 days per winter from the PPE mean for the historical period. The corresponding values  
418 for clear days weather are 15.0 days and 15.2 days per winter for ERA-5 and PPE, respectively.

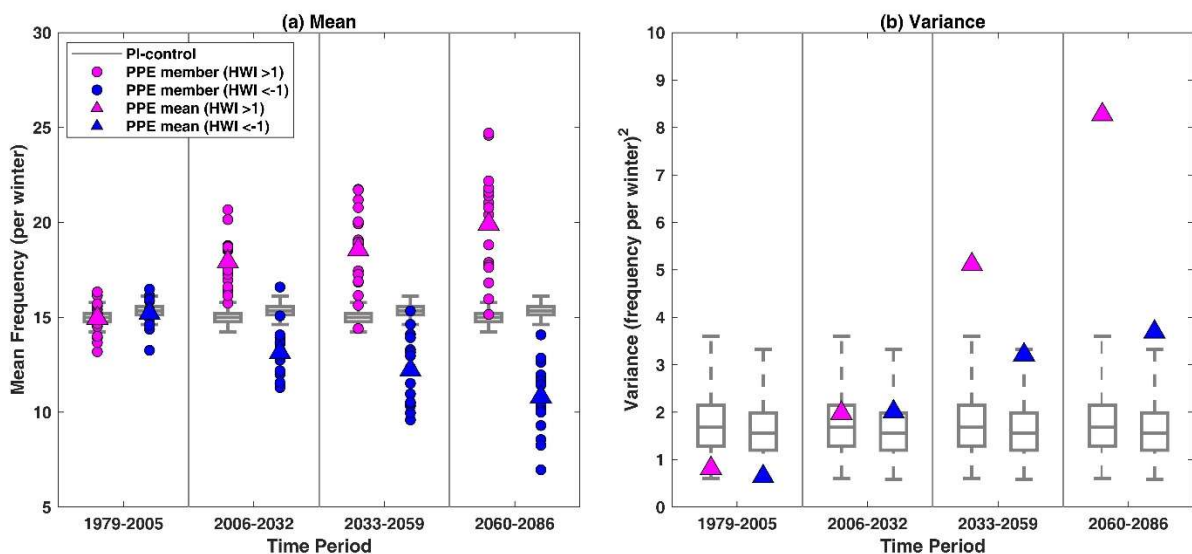
419 This shows a good agreement between the mean frequencies of [hazy haze conducive](#) and clear  
 420 [days](#) for the ERA-5 data and the PPE mean for the historical period.



421  
 422 **Figure 45** Frequency of [hazy \(haze conducive weather \(HWI>1, pink line\)](#) and clear [days \(weather](#)  
 423 [\(HWI<-1, blue line\)](#) per winter from ERA-5 reanalysis (1979 to 2018). Year 1979 represents period  
 424 from 1 December 1979 to 28 February 1980 and so on. For each winter (DJF), we calculate the total  
 425 number of [hazy days with HWI >1 as proxy for haze conducive weather](#) and [clear days with HWI < -1](#)  
 426 [as proxy for clear weather conditions](#). Grey lines show frequencies from 16 individual PPE members  
 427 and black line shows the mean of frequency using all 16 PPE members for 1969-2087 under the RCP8.5  
 428 scenario. Linear trend is calculated using [the](#) line of best fit.

429 The mean [frequency of haze conducive weather for near, mid and far future is 17.9,](#)  
 430 [18.6 and 19.9, respectively. The mean frequency for the same future periods for clear weather](#)  
 431 [is 13.2, 12.2 and 10.8, respectively \(Fig. 6a\). The mean change in the frequency of hazy days](#)

432 averaging haze conducive weather averaged across all PPE members is 2620%, 24% and 33%  
 433 for the near, mid and far future respectively as compared to the historical period, suggesting  
 434 that the frequency of hazy days haze conducive weather will likely increase for all future  
 435 periods (Fig. 5)-6a). However, there exists a very large range in the projected change for all  
 436 three future periods suggesting internal variability or parametric effect could influence the  
 437 future projections of haze conducive weather. For the near and mid future, hazy days with  
 438 HWI>1 are projected to change by -81% to 6541% and -12% to 65% across the 16 PPE  
 439 members, respectively, as compared to the frequency for the historical period. For the far  
 440 future, the range of projected change is even larger, and an increase of ~87% in the frequency  
 441 of hazy days haze conducive weather is also possible. It should be is noted that, for all three  
 442 periods, only one of the sixteen ensemble members suggests a decrease(E16 shown in daily  
 443 haze-Fig. 10) shows a reduction in the haze conducive weather frequency. whereas other  
 444 ensemble members show an increase in frequency for all periods. For the historical period, E16  
 445 ensemble member has a mean frequency of 16.3, which reduces to 16.2, 14.4 and 15.2 for near,  
 446 mid and far future. While E16 ensemble member shows a consistent reduction in mean  
 447 frequency in future, the reduction is specific to only this ensemble member and is not a general  
 448 feature across PPE members.



449



450 Figure 6 (a) Mean frequency of haze conducive weather (HWI>1, pink) and clear weather (HWI<-1,  
451 blue) for the historical period (1979-2005), near (2006-2032), mid (2033-2059) and far (2060-2086)  
452 future under the RCP8.5 scenario. Circles represent PPE members and triangles PPE mean. Grey box  
453 and whiskers show the distribution of 10,000 values of mean frequencies sub-sampled from the control  
454 simulation, (b) same as (a) but shows variance across 16 PPE members for each period. For box and  
455 whiskers, we first randomly sampled 10,000 time series of length 27 years using 2704 years of pre-  
456 industrial control simulation and calculated 10,000 values of mean frequency. We then randomly sub-  
457 sample 16 mean values (corresponding to the number of ensemble members) from the 10,000 mean  
458 values, calculated their mean for (a) and variance for (b). This is repeated 10,000 to obtain a distribution.  
459 The boxes are at the 25<sup>th</sup> and 75<sup>th</sup> percentile and the whiskers at 2.5<sup>th</sup> and 97.5<sup>th</sup> percentile of mean and  
460 variance distribution. For panel (a), the box and whiskers are comparable only to the ensemble means  
461 (triangles) and not ensemble members (circles).

462 For clear weather (HWI<-1), the mean change in the frequency averaging across all  
463 PPE members is -2113%, -20% and -29% for near, mid and far future, respectively (Fig 56a).  
464 Considering the range across the 16 PPE members, the frequency of clear weather for near,  
465 mid and far future is projected to change by -4029% to 925%, -36% to 10% and -57% to -9%,  
466 respectively. Overall, most ensemble members show an increase in the frequency of hazy  
467 dayshaze conducive weather and a reduction in the frequency of clear daysweather for all three  
468 future periods however. However, negligible change or even the opposite change, though less  
469 likely, but possible for all periods.

470 Figure 6 Frequency of winter hazy days versus clear days We also determine the influence  
471 of anthropogenic climate change and the parametric effect on the frequencies of haze conducive  
472 weather (HWI>1) and clear weather (HWI<-1) for the historical as well as the three future  
473 periods. As shown in later Section 5, the estimate of interannual variance from the control is  
474 representative of all time periods and shows no discernible parametric effect. Therefore, we  
475 pool the 16 PPE control simulations to sample the internal variability for box and whiskers  
476 shown in Fig. 6 (a) and 6 (b) (see captions for details on resampling).

477 In Fig. 6 (a), we show the mean frequency of haze conducive weather and clear weather  
478 for 16 individual PPE members (circles) and PPE mean (triangles). The grey box and whiskers  
479 represent the range of ensemble mean frequencies that can be explained by the internal

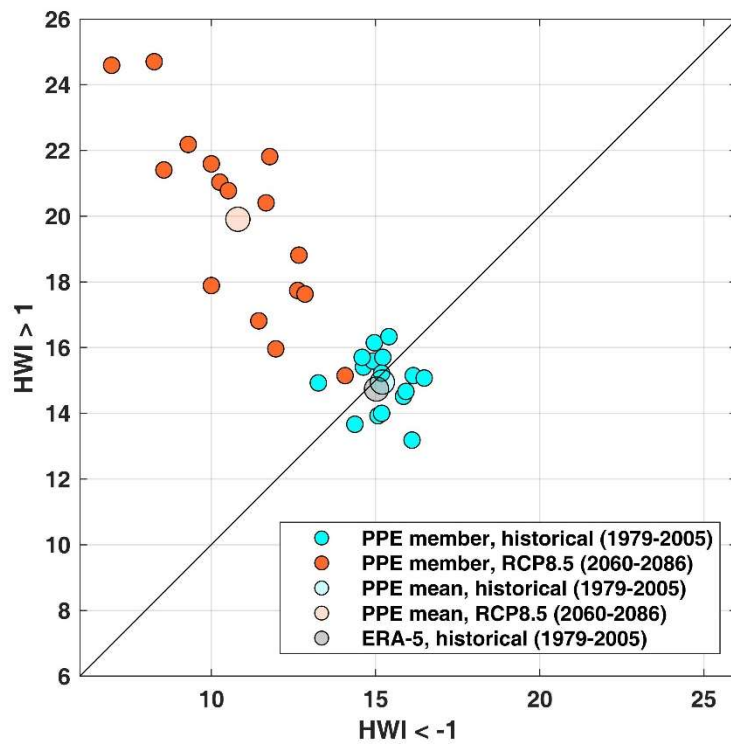
480 variability. If the PPE mean (triangles) lies within the whiskers (i.e. 95 percentile of the control  
481 distribution) we conclude no influence of anthropogenic climate change on mean frequency  
482 however if the PPE mean lies outside the whiskers, it would represent a climate change signal  
483 in the mean frequency. Figure 6 (a) suggest that the mean frequencies for haze conducive as  
484 well as clear weather lies within the box-whiskers for the historical but lies outside the whiskers  
485 for the three future periods, thereby showing a clear impact of anthropogenic climate change  
486 on the frequencies of both haze conducive and clear weather conditions.

487 \_\_\_\_\_ We now examine whether the differences in the mean frequency across different PPE  
488 members (shown by circles in Fig. 6a) for a given period can be explained by the internal  
489 variability or if the differences in PPE members partly arise due to the parametric effect. The  
490 triangles in Fig. 6b shows the variance across 16 PPE members, i.e. variance across 16 circles  
491 shown in Fig. 6a, for each time period. The whiskers in Fig. 6b show the 95<sup>th</sup> confidence  
492 interval from the control simulation and is representative of the internal variability. For any  
493 time period, if the PPE member variance (triangle) lies within the whiskers, we conclude that  
494 the differences in mean frequencies in Fig. 6a can be fully explained by the internal variability  
495 and there is no discernible impact of the parametric effect. However, if the triangles lie outside  
496 the whiskers in Fig. 6b, we conclude an impact of the parametric effect on the mean frequency  
497 for that period. For the points that lie outside the whiskers in Fig. 6b, we also quantify the  
498 percentage of variance that can be explained by the internal variability and parametric effect.  
499 For any time period, the variance in ensemble mean due to the parametric effect is simply  
500 calculated as follow and the remaining variance is attributed to the internal variability.

501 
$$\frac{\text{Total variance in the ensemble mean} - \text{Mean variance from the control simulation}}{\text{Total variance in the ensemble mean}} \times 100$$

502 \_\_\_\_\_ Figure 6b shows that the variance in PPE mean frequency for historical and future  
503 periods lies within the range sampled by the internal variability for both haze conducive

504 [weather \(HWI>1\) and clear weather \(HWI<-1\)](#). For mid-future, the variance in haze conducive  
 505 [weather lies outside the whiskers and whereas the variance for clear weather lies within the](#)  
 506 [whiskers. For mid-future and for haze conducive weather, the internal variability can explain](#)  
 507 [~33% of the variance across PPE members and the remaining ~67% arises due to the parametric](#)  
 508 [effect. For the far future, triangles corresponding to both haze conducive and clear weather lies](#)  
 509 [well outside the whiskers and therefore show a clear influence of parametric effect. Only ~20%](#)  
 510 [of the variance in the frequency of haze conducive weather and ~43% variance in the frequency](#)  
 511 [of clear weather can be explained by the internal variability and the remaining 80% and 57%](#)  
 512 [respective variance in the frequencies arise due to the parametric effect.](#)



513

514 **Figure 7** [Frequency of haze conducive weather \(HWI>1\) versus clear weather \(HWI<-1\)](#) averaged over  
 515 the historical period (1979-2005) and the far-future (2060-2086) period under RCP8.5 using all PPE  
 516 members. Circles denote individual PPE members whereas triangles denote the mean of the members.  
 517 Grey triangle shows mean frequency from ERA-5 reanalysis for the historical period (1979-2005). The  
 518 black solid line shows the 1:1 (identity) line.

519 In addition to the changes in the frequencies over time, we also investigate the relative  
 520 changes in the frequency of [hazy days](#) [haze conducive weather \(HWI>1\)](#) versus clear [days for](#)



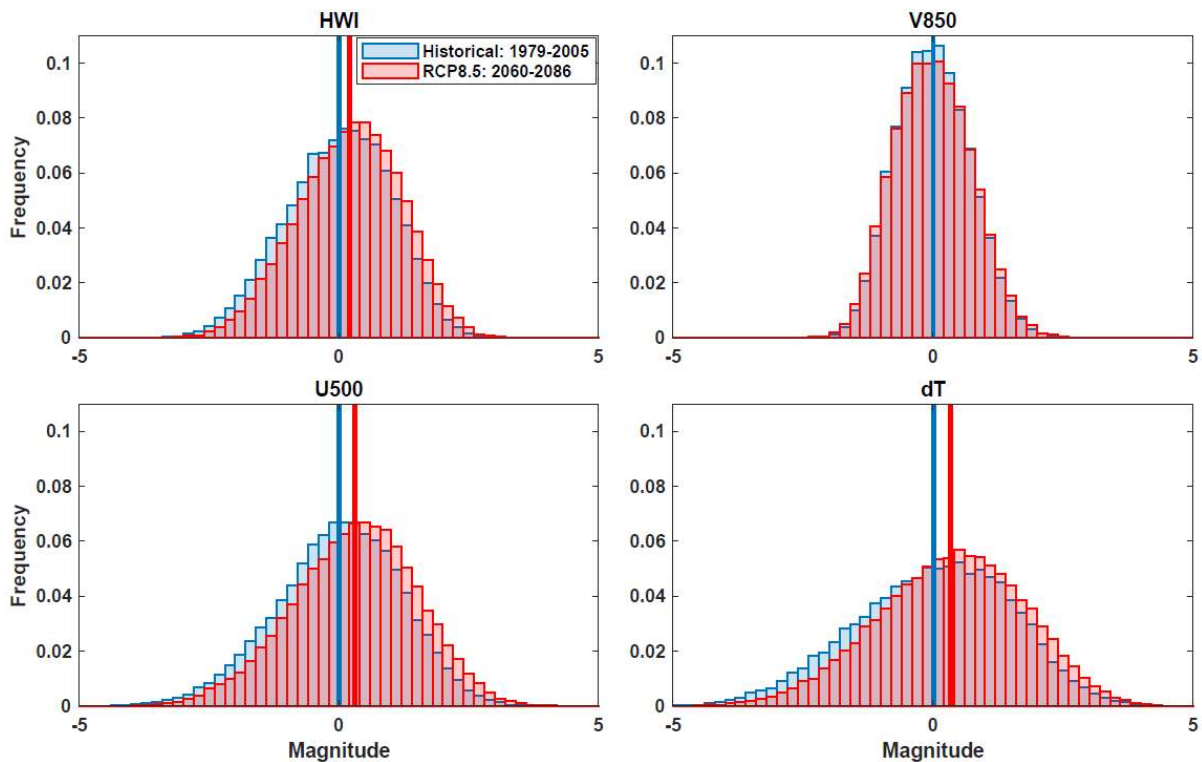
521 ~~a given winter weather (HWI<-1)~~. The average ~~frequency of hazy days~~~~haze conducive~~ and  
522 clear ~~days weather frequency~~ over the historical period are almost equal for each PPE member  
523 (Fig. ~~6~~. ~~7~~). All PPE members show ~~a higher frequency of hazy days~~~~for haze conducive weather~~  
524 than clear ~~days weather~~ under the far future (2060-2085), however, there exists a substantial  
525 range in this change. The frequency of winter haze ~~days conducive weather~~ can be similar or  
526 up to 3.5 times the frequency of clear ~~days weather conditions~~ (Fig. ~~6~~~~7~~). Similar results are also  
527 obtained for ~~the~~ near and mid-future. Averaged across the PPE members, the number of  
528 ~~hazy haze conducive~~ days can increase by ~2 times as compared to the number of clear days in  
529 future. As noted in Fig. ~~6~~~~7~~, the spread in the ~~haze conducive weather~~ ~~frequency of hazy days~~  
530 amongst individual ensemble members is also larger for the far future (2060-2086) compared  
531 to the historical period. This suggests a larger uncertainty and a larger range of possible future  
532 meteorological conditions affecting haze and air quality as compared to the historical period.

533 Other studies have (e.g., Cai et al., 2017; Callahan and Mankin, 2020) also found similar  
534 increases in the frequency of ~~hazy days~~~~haze conducive weather~~ for the future. However, the  
535 range of projected change ~~differ differs~~ substantially across models as well as ensemble  
536 members. In our study, in addition to the frequency of ~~hazy days~~~~haze conducive weather~~, we  
537 also evaluate the changes in the frequency of clear ~~days weather~~ across different future periods  
538 and compared the relative changes in both the frequencies, which is not examined in the past  
539 studies.

## 540 **5. Role of individual meteorological variables**

541 We now investigate ~~the role of individual constituent meteorological variables in~~  
542 ~~driving the~~ changes in the ~~distribution of the HWI as well as individual constituents of the~~ HWI  
543 between the far-~~future~~ (2060-86) and the historical (1979-2005) period. The probability  
544 distribution of the HWI shows a shift in the distribution towards higher magnitudes for the far-  
545 future as compared to the historical period (Fig. 8). This implies an increased frequency ~~in~~

546 hazy of haze conducive weather, as the number of days, as values with  $HWI > 1$  increase. A  
 547 similar shift is apparent in the zonal-mean wind ( $U_{500}$ ) and the vertical temperature profiles  
 548 ( $dT$ ), whereas no apparent shift is noted in  $V_{850}$  suggesting a relatively less important role of  
 549  $V_{850}$  in driving the future changes in the  $HWI$ . We also find that the shift in the  $HWI$ , as well  
 550 as  $U_{500}$  and  $dT$  distribution, is not due to the shift in one particular PPE member or time period.  
 551 It is consistent across the 16 PPE members and is continual over time from the historical to the  
 552 far-future period. Therefore, for the PPE analysed here, the changes in the haze conducive  
 553 weather ( $HWI > 1$ ) is largely associated with the changes in the  $U_{500}$  and  $dT$ , and  $V_{850}$  appear to  
 554 have a less important role. Despite using a multimodel ensemble and a different time-period  
 555 than used here, a similar result with a relatively larger shift in the PDFs of  $U_{500}$  and  $dT$  as  
 556 compared to  $V_{850}$  can also be noted in the Cai et al. (2017).



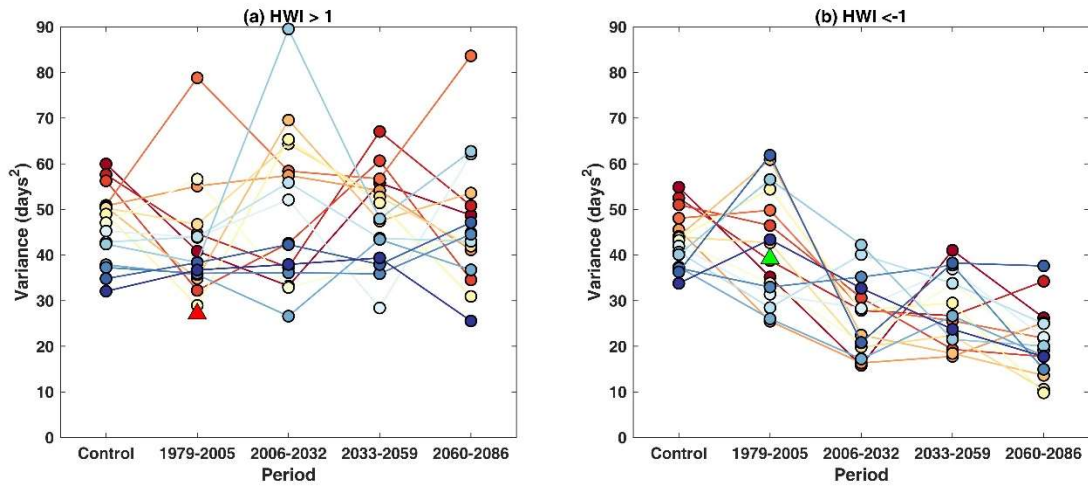
557  
 558 **Figure 78** Probability Distribution Functions (PDF) for the winter  $HWI$ , meridional winds at  
 559 850 hPa pressure level ( $V_{850}$ ), zonal winds at 500 hPa pressure level ( $U_{500}$ ) and temperature  
 560 gradient between the lower and upper troposphere ( $dT$ ). The PDF for the  $HWI$  is created using  
 561 the daily DJF time series of all 16 PPE members. PDFs for  $V_{850}$ ,  $U_{500}$  and  $dT$  are created using  
 562 daily DJF values the normalized daily DJF time series of each variable calculated for the  $HWI$

563 (see section 2.2 for details) and represents the constituent variables of the HWI. Blue bars  
564 show the PDFs for the historical (blue)period and red for the far- future (red) under the RCP  
565 8.5 by pooling in all 16 PPE members.scenario. Blue and red solid lines show the mean values  
566 of the PDF for historical and far future, respectively.

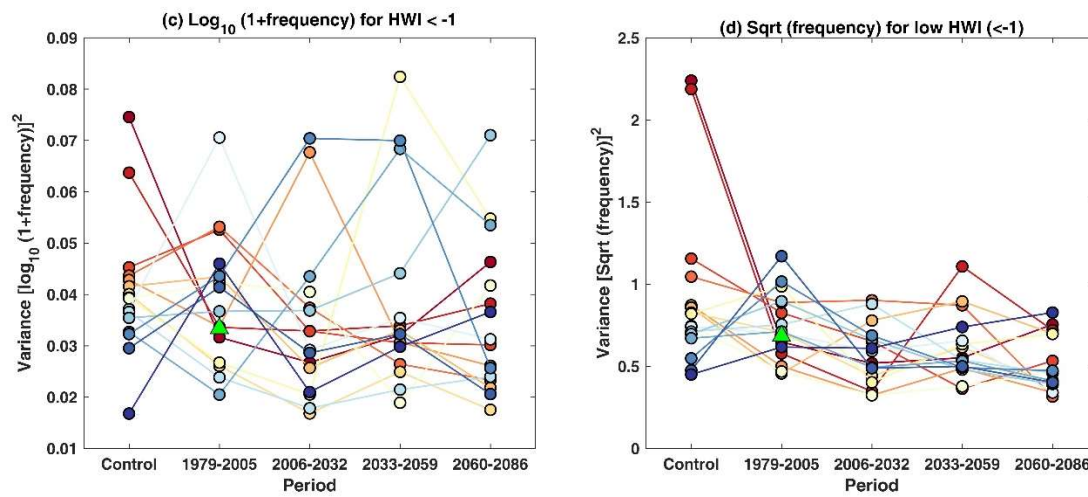
567 **65. Interannual variability in ~~the frequency of hazyhaze conducive~~ and clear weather**  
568 **conditionsfrequency**

569 Large interannual variability in the frequency of hazyhaze conducive (HWI>1) and  
570 clear daysweather (HWI<-1) is apparent in both individual PPE members and ERA-5  
571 reanalysis (Section 4). Therefore, we examine the changes in the interannual variance of the  
572 frequencies for future periods as compared to the historical period. We also compare the  
573 variance in historical and future time-periods with the variance in the control simulation to  
574 discern the influence of the model physical parameterisations, i.e. parametric effect, on the  
575 variance.

576 ~~The interannual variance for ERA-5 data is 27 days<sup>2</sup> and 39 days<sup>2</sup> for hazy and clear~~  
577 ~~days, respectively, for the historical period (1979-2005) (triangles in Fig. 8a-b). The~~  
578 ~~interannual variance in the frequency of hazy days derived from the PPE members for the~~  
579 ~~historical period is larger than that for the ERA-5, whereas for the clear days the variance for~~  
580 ~~ERA-5 lies within the range of the PPE members. No consistent change in the interannual~~  
581 ~~variance of hazy days is noted for any of the PPE members (note the changes in colour ranking)~~  
582 ~~from the historical to the future periods suggesting little influence of the parametric effect on~~  
583 ~~the interannual variance of hazy days.~~



584



585

586 **Figure 89** Interannual variance in frequency of winter (a) [hazyhaze conducive weather \(HWI>1\)](#) and  
 587 (b) [clear daysweather \(HWI<-1\)](#) for the control simulation, historical (1979-2005), and near (2006-  
 588 2032), mid (2033-2059) and far-future (2060-2086) under RCP8.5 for all 16 PPE members. Coloured  
 589 circles are for individual PPE members and triangles for ERA-5 reanalysis. (c-d) are same as (b) but  
 590 with log<sub>10</sub> and square root power transformations. For (c-d), we first calculate the log<sub>10</sub> of (1+frequency)  
 591 and square-root of the frequency of clear days for the control simulation and each time-period, and then  
 592 estimate variance for each respective period. The length of control simulation and all future periods is  
 593 the same as historical, i.e. 27 years. The 27 years used for control here are randomly selected from 170-  
 594 year control simulation for each member.

595 [The interannual variance for ERA-5 data is 27 days<sup>2</sup> and 39 days<sup>2</sup> for haze conducive](#)  
 596 [and clear weather, respectively, for the historical period \(1979-2005\) \(triangles in Fig. 9a-b\).](#)  
 597 [The interannual variance in haze conducive weather frequency derived from the PPE members](#)  
 598 [for the historical period is larger than that for the ERA-5, whereas for the clear weather the](#)  
 599 [variance for ERA-5 lies within the range of the PPE members. No consistent change in the](#)

600 [interannual variance of haze conducive weather is noted for any of the PPE members \(note the](#)  
601 [changes in colour ranking\) from the historical to the future periods suggesting little influence](#)  
602 [of the parametric effect on the interannual variance of haze conducive weather.](#)

603 In contrast, the frequency of clear [daysweather](#) for most PPE members show a marked  
604 reduction in the interannual variance from historical to near-future (Fig. [8b9b](#)). However, as  
605 the frequency of clear [daysweather](#) show a decreasing trend in time (see Fig. [4b5b](#)), the mean  
606 frequency would be expected to reduce for the three future periods. Also, the reduction in  
607 variance could arise as the frequencies of clear [daysweather](#) approach their lower bound of  
608 zero. With count data, a power transformation is often applied to stabilize the variance across  
609 all time periods. We ~~tried~~[applied](#) two power transformations, i.e.  $\log_{10}(1+x)$  and square-root  
610 ( $x$ ), where  $x$  is the count data (Fig. [8e9c-d](#)). We find the spread in the variance in the control  
611 simulation across the PPE members is comparable with the historical as well as future periods  
612 (Fig. [8e9c-d](#)). Note that for control simulation we randomly selected 27 years (length same as  
613 historical and future periods) from 170 years of control simulation from each PPE member,  
614 however, we note comparable variance for the other randomly selected samples. Figure [89](#) (c-  
615 d) also shows that the individual PPE members show inconsistent changes in the variance  
616 (noting changes in the colour ranking) from control to historical and future periods. Therefore,  
617 no robust changes in the interannual variance of ~~hazy or  $\log_{10}(1+$  frequency of~~ [haze conducive](#)  
618 [and clear ~~days~~weather](#) can be detected from control to historical and future periods. This  
619 means we can use the variance in the control simulation as a representative estimate of internal  
620 variability. This enables us to quantify the influence of the parametric effect and anthropogenic  
621 climate change on the [mean frequencies \(see previous section\) and trends in frequencies \(see](#)  
622 [next section\)](#) across ~~the~~ different periods ~~(see next section).~~

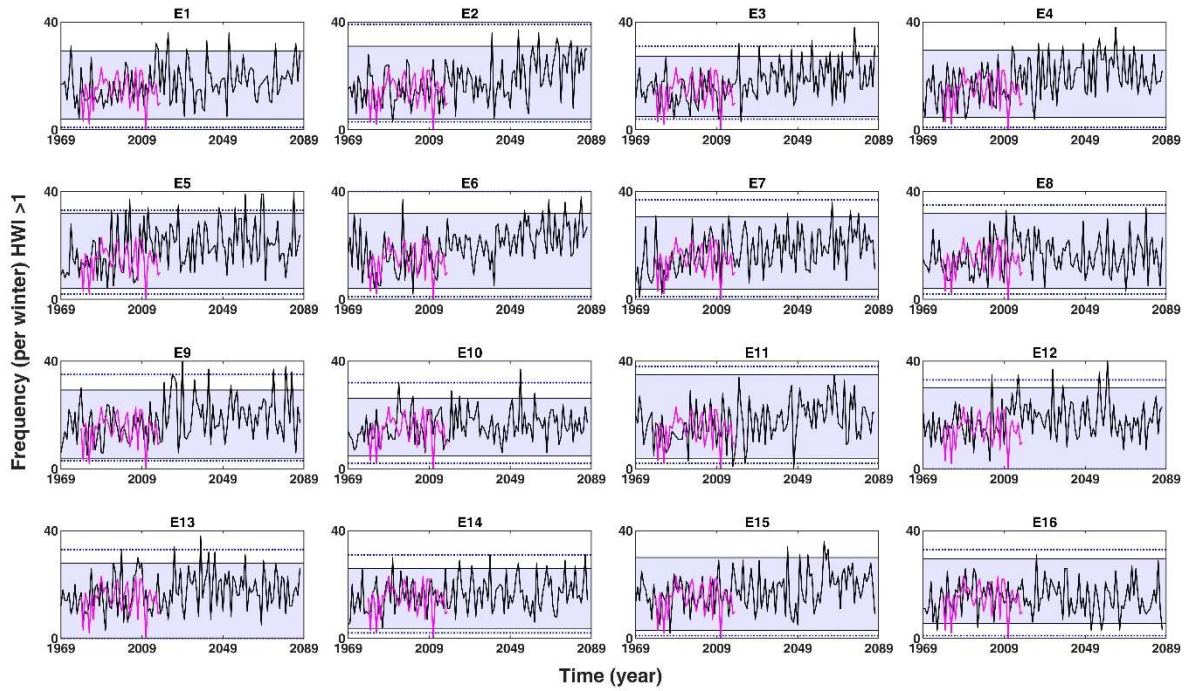
623 **[76. Influence of the parametric effect and anthropogenic climate change and parametric](#)**  
624 **[effect on trends](#)**

625 We discern the influence of the ~~parametric effect and~~ anthropogenic climate change and  
626 parametric effect on the future projections of the trends in the frequency of hazyhaze conducive  
627 weather (HWI >1) and clear ~~days~~. ~~Figure 9 shows the~~ weather (HWI <-1). The time series of  
628 the ~~frequency of winter~~ hazyhaze conducive and clear ~~days~~ weather frequency from ERA-5  
629 and the 16 PPE members for the historical and future periods ~~is shown in Fig. 11 (a) and 11~~  
630 (b). The 95<sup>th</sup> percentile values (blue shaded region) and the range (blue dotted lines) in the  
631 frequency of hazyhaze conducive and clear ~~days~~ weather frequency from the respective control  
632 simulation for each PPE member are also shown.

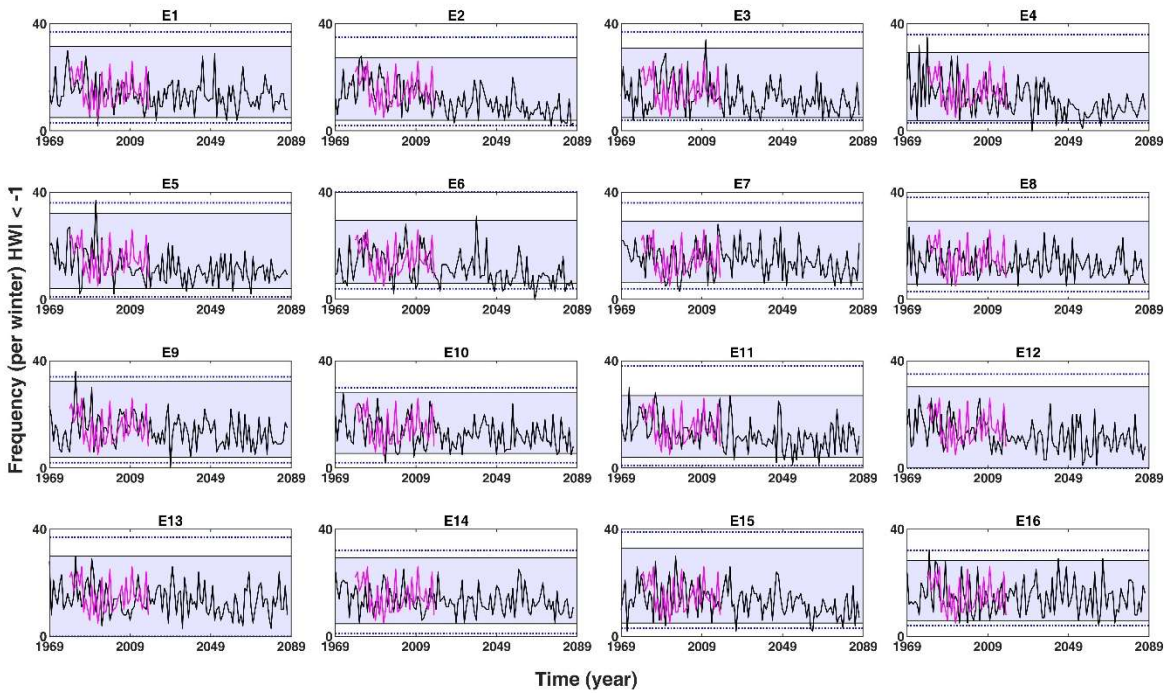
633 For ~~hazy days~~ haze conducive weather (HWI>1), the time series for selected PPE  
634 members (e.g. E3, E4) show increasing positive trends. In particular, towards the end of the  
635 21<sup>st</sup> century (Fig. 9a10a), the lower half of the control range is seldom sampled and more than  
636 the expected number of values lie above the 97.5<sup>th</sup> percentile of the control frequencies. In  
637 contrast, for other PPE members (e.g. E8, E10), the full time series sample the control  
638 distribution evenly throughout the full period. For clear ~~days~~ weather (HWI<-1), some  
639 members (e.g. E3, E4) show a clear reduction during the 21<sup>st</sup> century whilst others (e.g. E16)  
640 show ~~that~~ no trend and explore the control distribution evenly (Fig 9b10b).

641 ~~———— We first examine ————~~ In Section 4, we examined the influence of ~~the~~ anthropogenic  
642 climate change and parametric effect on the mean frequencies. The analysis of mean  
643 frequencies provides an estimate of the accumulated influence of climate change on  
644 frequencies with respect to the control simulations whereas analysis of trends would provide a  
645 better estimate of changes within a selected time period. Therefore, we apply the same analysis  
646 on the trends in the frequencies (Fig. 11).





647



648

649 **Figure 10** Frequency of (a) haze conducive weather ( $HWI > 1$ ) and (b) clear weather ( $HWI < -1$ ) per  
 650 winter for individual PPE members (black line) under the historical and RCP8.5 scenarios for 1969-  
 651 2087 and ERA5 reanalysis (pink line) for 1979-2018. Blue shaded region shows the 95<sup>th</sup> confidence  
 652 interval and blue dashed line shows the range of the frequency of hazy and clear days. A haze  
 653 conducive and clear weather for the pre-industrial control simulation of 170-years.

654 We calculate the ensemble mean trend obtained from the 16 individual PPE member  
655 trends to determine the influence of climate change for the historical period (see captions of  
656 Fig. 11 for details). We describe the evolution of the historical trend for three equal-length  
657 future time periods (i.e. near, mid and far future) and examine if the historical trends are  
658 sustained across the 21<sup>st</sup> century and if the trends are discernible outside the range described  
659 by the internal variability (Fig. 11a-b). The grey whiskers in Fig. 11 (a) and (b) cover the range  
660 of trends that can be noted in section 6, for hazy days and  $\log_{10}(1+\text{explained by internal$   
661 variability and any trend values lying outside the grey whiskers represent the influence of  
662 anthropogenic climate change.

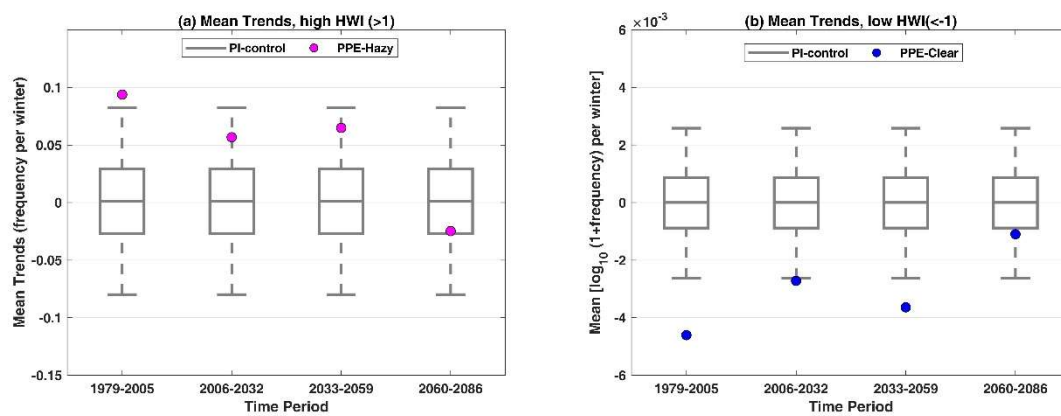
663 The mean trend in the frequency of clear days), the estimate of interannual variance  
664 from the control is representative of all time periods and shows no discernible both haze  
665 conductive (HWI>1) and clear weather (HWI <-1) for the historical period (1979-2005) lie  
666 outside the 95% confidence interval of the control simulations. This suggests that the trends  
667 noted for the historical period cannot be explained by internal variability alone and there is a  
668 substantial impact of anthropogenic climate change on the historical trends. The trends in haze  
669 conductive weather lie within the envelope of internal variability for the three future periods  
670 analysed here implying that the historical trend is not sustained over the 21<sup>st</sup> century and  
671 indistinguishable from the internal variability for the future. Figure 11 (a) also shows a positive  
672 mean trend in haze conducive weather (HWI>1) for historical, near and mid future, but a weak  
673 negative trend for far future. While the frequency of haze conducive weather increases for all  
674 three future periods with respect to the historical period as shown in Fig. 6a, the trends only  
675 show an increment or reduction for that period as these are not referenced to the historical  
676 period. Therefore, trends could still be negative within any selected period, as in the case of  
677 the far future. In contrast, the mean trends in clear weather frequency for near (2006-2032) and  
678 mid future (2033-2059) lie outside the 95% confidence interval of the control simulation. This



679 [shows that for clear weather frequency \(HWI<-1\), the historical trend is sustained over the first](#)  
 680 [half of the 21<sup>st</sup> century and then it levels off.](#)

681 [We now examine the influence of the parametric effect. Therefore, we pool on the 16](#)  
 682 [PPE control simulations to sample trends in the internal variability. frequency of haze conducive](#)  
 683 [and clear weather.](#) In Fig. [10\(a-b\)11 \(c\) and \(bd\)](#), we show the variance in trends for the time  
 684 series resampled using the control simulation (see captions for details on resampling). The grey  
 685 box and whiskers show the 95<sup>th</sup> confidence interval of the control variance used to represent  
 686 the internal variability. The variance in PPE trends calculated using 16 PPE members for  
 687 selected time periods is overlaid (circles). In Fig. [10\(a-b\)11 \(c-d\)](#), if the variance for historical  
 688 or future periods lies outside the whiskers, we conclude an impact of the parametric effect on  
 689 the trends. [However, if the variance across the 16 PPE members lies within the whiskers, we](#)  
 690 [conclude no impact of the parametric effect on the trend.](#) Note that the variance in trends for  
 691 clear [daysweather](#) is in log-transformed space. As can be seen in Fig. [10a11c](#) and [10b11d](#), the  
 692 variance in PPE trends for historical and future periods lies within the [envelope95<sup>th</sup> percentile](#)  
 693 [distribution](#) of the internal variability for both [hazyhaze conducive](#) and clear [daysweather](#).  
 694 Therefore, we do not find any discernible influence of the parametric effect on the trends in the  
 695 [frequency of hazy and clear daysfrequencies.](#)

696



701  
702

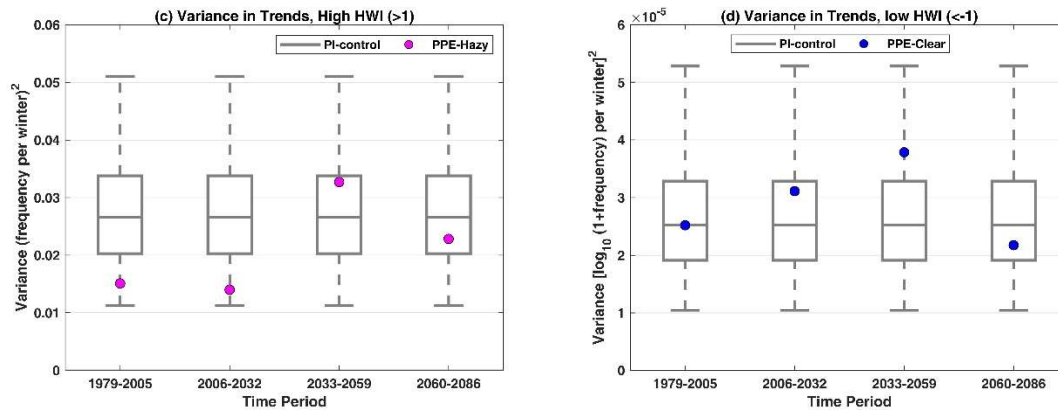


**Figure 10** Variance in Mean PPE trends for the frequency of winter (a) hazy haze conducive weather ( $HWI > 1$ ) and (b) clear days weather ( $HWI < -1$ ) for winter. Circles show the variance in mean trends from 16 PPE members for the historical (1979-2005) and near (2006-2032), mid (2033-2059) and far (2060-2086) future under the RCP8.5 scenario. Grey box and whiskers show the distribution of 10,000 values of variance in trends sub-sampled from the control simulation. (c-d) same as (a-b) but variance mean is replaced by mean variance in trends. For box and whiskers, we first randomly sampled 10,000 time series of length 27 years using 2704 years of pre-industrial control simulation and calculated 10,000 values of trends. We then randomly sub-sample 16 trends values from the 10,000 trend values and calculate the variance and mean of 16 trend values. The boxes are at the 25<sup>th</sup> and 75<sup>th</sup> percentile and the whiskers at 2.5<sup>th</sup> and 97.5<sup>th</sup> percentile of mean and variance distribution. For clear days, the frequencies were transformed to log space by applying a power transformation of  $\log_{10}(1 + \text{frequency})$  before calculating trends.

We now examine the influence of anthropogenic climate change on the trends in the frequency of hazy and clear conditions. We calculate the mean trend obtained from the 16 individual PPE member trends (Fig. 10c-d), to determine the influence of climate change across selected time periods. The grey whiskers in Fig. 10 (c) and (d) cover the range of trends that can be explained by internal variability and any trend values lying outside the grey whiskers represent the influence of anthropogenic climate change.

The mean trend in the frequency of both hazy and clear days for the historical period (1979-2005) lie outside the 95% confidence interval of the control simulations, suggesting a substantial impact of anthropogenic climate change on the historical trends in the PPE. Similarly, the mean trends for clear days for near (2006-2032) and mid future (2033-2059) lie outside the 95% confidence interval of the control simulation. Thus, we find the impact of the

728 ~~climate change on both hazy and clear days. However, it is only discernible for specific periods~~  
729 ~~due to the underlying large internal variability in the frequency of hazy and clear days.~~

## 730 **87. Conclusions**

731 In this study, we elucidate for the first time the influence of model physical  
732 parametrisations, in addition to internal variability and climate change, on the future ~~hazyhaze~~  
733 ~~conductive~~ and clear weather conditions over the North China Plain (NCP) using the Perturbed  
734 Parameter Ensemble (PPE) from the Met Office HadGEM3-GC3.05 model. We ~~use a~~  
735 ~~meteorology-based daily Haze Weather Index (HWI), which has been previously used by a~~  
736 ~~number of studies to~~ examine the ~~changes in~~ winter (December-February) haze ~~conductive and~~  
737 ~~clear~~ weather conditions ~~for past and future~~ over ~~Beijing-the~~ NCP using a large-scale  
738 ~~meteorology-based daily Haze Weather Index (HWI)~~. We first identify the regional extent of  
739 the application of the HWI over China. We find that the  $HWI \geq 1$  can be used as an indicator  
740 of ~~hazy and~~ ~~haze conductive weather conditions and~~  $HWI < -1$  as an indicator of clear weather  
741 conditions for the entire NCP due to the spatial coherence of regional meteorological conditions  
742 over this region.

743 The PPE shows that under the RCP8.5 ~~emission~~ scenario, the mean frequency of ~~hazy~~  
744 ~~dayshaze conductive weather (HWI>1)~~ can increase by up to ~65% in ~~the~~ near (2006-2032) and  
745 mid (2033-2059) future and by ~87% in far-~~future~~ (2060-2086) as compared to the historical  
746 period (1979-2005). In contrast, the frequency of clear ~~daysweather (HWI<-1)~~ can reduce by  
747 up to ~40% in ~~the~~ near and mid-future and by ~57% in ~~the~~ far-~~future~~. However, the opposite  
748 change of relatively lower magnitude or negligible change in frequency of ~~hazyhaze conductive~~  
749 and clear ~~weather~~, though less likely, is possible. The absolute number of ~~hazy~~-days ~~forwith~~  
750 ~~haze conductive weather in~~ the far future can remain ~~the~~ same or up to ~3.5 times higher than  
751 the clear ~~days for any given winter~~-~~weather over the NCP~~. There also exist a large interannual

752 variability in the frequency of ~~hazy~~haze conducive and clear weather conditions. However, no  
753 systematic change in the interannual variance of the ~~frequency of hazy or clear days~~frequencies  
754 is ~~projected~~noted in future as compared to the historical period. We also find that the ~~future~~  
755 changes in ~~hazy or clear~~the haze conducive weather ~~conditions are largely influenced~~  
756 ~~by~~(HWI>1) for the future is associated with the changes in the mid-tropospheric zonal wind  
757 component and strong vertical temperature gradient between the lower to upper troposphere  
758 over the ~~North China Plain~~NCP. We ~~do not~~ find ~~any discernible a consistently growing~~  
759 influence of ~~the anthropogenic climate change and~~ parametric effect on the mean haze  
760 conductive and clear weather frequencies across the 21<sup>st</sup> century. This suggests that in addition  
761 to the internal variability, the parametric effect adds as an additional source of uncertainty in  
762 future projections of ~~trends in the frequency of hazy and clear days. However, we~~haze  
763 conductive and clear weather, particularly towards the end of the 21<sup>st</sup> century. We find that the  
764 impact of anthropogenic climate change ~~on the~~is discernible in trends for ~~both hazy and clear~~  
765 ~~days for the~~ historical ~~and specific future~~period for haze conducive weather and up to mid of  
766 the 21<sup>st</sup> century for clear weather. Beyond these periods, ~~suggesting climate change can~~  
767 ~~exacerbate the increase in the number of hazy and the reduction in the number of clear days in~~  
768 ~~future. the historical trends are not sustained and not distinguishable from the internal~~  
769 variability.

770 This study considers four atmospheric variables to examine the changes in future  
771 ~~hazy~~haze conducive and clear weather conditions, however, other atmospheric variables (e.g.,  
772 boundary layer height) or processes may ~~also~~ influence the ~~hazy or clear weather~~  
773 ~~conditions~~occurrence of haze. Furthermore, even though our study shows the potential for an  
774 increase in ~~hazy~~haze conducive weather conditions and a reduction in clear weather conditions  
775 for the future periods ~~examined using~~, the HWI, the actual formation of haze ~~also depends~~will  
776 depend on future emissions of air pollutants and their precursors. If the source emissions are

777 cut-off or reduced in the future, the risk of haze formation would naturally reduce.  
778 Nevertheless, the projections of changes in the frequency and interannual variance in haze  
779 conducive weather conditions can be very useful for developing successful adaptation and  
780 mitigation policies for the future that consider both emissions and climate change, and therefore  
781 can be beneficial for near and long-term planning and decision-making in relation to improving  
782 future PM<sub>2.5</sub> air quality.

### 783 **Data Availability**

784 The Copernicus Climate Change Service (C3S) (2017): ERA5: Fifth generation of ECMWF  
785 atmospheric reanalyses of the global climate data are available through Copernicus Climate  
786 Change Service Climate Data Store (CDS) (<https://cds.climate.copernicus.eu/>). The PM<sub>2.5</sub>  
787 concentrations for the US Embassy station in Beijing are archived at the following website  
788 (<http://www.stateair.net/web/historical/1/1.html>). The haze weather index time series for PPE  
789 and visibility data used in this paper can be obtained from the authors. The CAQRA dataset  
790 can be freely downloaded at <https://doi.org/10.11922/sciencedb.00053>.

### 791 **Author Contribution**

792 SJ and RMD conceived and designed the manuscript; DS conducted PPE simulations using  
793 Met Office HadGEM model; LP provided the visibility data; SJ performed data analysis,  
794 produced figures, wrote the first draft; all co-authors provided comments on the manuscript  
795 and contributed to writing.

### 796 **Competing interests**

797 The authors declare no financial or non-financial conflict of interest.

### 798 **Acknowledgements**

799 We thank Dr Li Ke for [the](#) discussion on the HWI calculation and Dr Peiqun Zhang for [the](#)  
800 discussion on severe haze episodes in China. This work and its contributors (SJ, RMD, DS,  
801 ST, ZS) were supported by the UK-China Research & Innovation Partnership Fund through  
802 the Met Office Climate Science for Service Partnership (CSSP) China as part of  
803 the Newton Fund (Met Office Reference Number: DN37368). RD and ZS also acknowledge  
804 NERC for funding under the Atmospheric Pollution and Human Health Programme: Grant  
805 Nos. NE/N006941/1 and NE/N007190/1. CL was supported by the National Key Research and  
806 Development Program of China (Grant No. 2018YFA0606501). [We also thank the two](#)  
807 [reviewers for their constructive comments and suggestions on this manuscript.](#)

## 808 **References**

- 809 An, Z., Huang, R. J., Zhang, R., Tie, X., Li, G., Cao, J., Zhou, W., Shi, Z., Han, Y., Gu, Z., and  
810 Ji, Y.: Severe haze in northern China: A synergy of anthropogenic emissions and  
811 atmospheric processes, *Proc Natl Acad Sci U S A*, 116, 8657-8666,  
812 10.1073/pnas.1900125116, 2019.
- 813 Bai, N., Khazaei, M., van Eeden, S. F., and Laher, I.: The pharmacology of particulate matter  
814 air pollution-induced cardiovascular dysfunction, *Pharmacology & therapeutics*, 113, 16-  
815 29, 2007.
- 816 Cai, W., Li, K., Liao, H., Wang, H., and Wu, L.: Weather conditions conducive to Beijing  
817 severe haze more frequent under climate change, *Nature Climate Change*, 7, 257-262,  
818 10.1038/nclimate3249, 2017.
- 819 Callahan, C. W., Schnell, J. L., and Horton, D. E.: Multi-index attribution of extreme winter  
820 air quality in Beijing, China, *Journal of Geophysical Research: Atmospheres*, 124, 4567-  
821 4583, 2019.

822 Callahan, C. W., and Mankin, J. S.: The Influence of Internal Climate Variability on Projections  
823 of Synoptically Driven Beijing Haze, *Geophysical Research Letters*, 47,  
824 10.1029/2020gl088548, 2020.

825 Chen, H., and Wang, H.: Haze days in North China and the associated atmospheric circulations  
826 based on daily visibility data from 1960 to 2012, *Journal of Geophysical Research:*  
827 *Atmospheres*, 120, 5895-5909, 2015.

828 Deser, C., Knutti, R., Solomon, S., and Phillips, A. S.: Communication of the role of natural  
829 variability in future North American climate, *Nature Climate Change*, 2, 775-779, 2012.

830 Deser, C., Phillips, A. S., Alexander, M. A., and Smoliak, B. V.: Projecting North American  
831 climate over the next 50 years: Uncertainty due to internal variability, *Journal of Climate*,  
832 27, 2271-2296, 2014.

833 Han, Z., Zhou, B., Xu, Y., Wu, J., and Shi, Y.: Projected changes in haze pollution potential in  
834 China: an ensemble of regional climate model simulations, *Atmospheric Chemistry and*  
835 *Physics*, 17, 10109-10123, 10.5194/acp-17-10109-2017, 2017.

836 Hawkins, E., and Sutton, R.: Time of emergence of climate signals, *Geophysical Research*  
837 *Letters*, 39, n/a-n/a, 10.1029/2011gl050087, 2012.

838 He, J., Yu, Y., Xie, Y., Mao, H., Wu, L., Liu, N., and Zhao, S.: Numerical model-based  
839 artificial neural network model and its application for quantifying impact factors of urban  
840 air quality, *Water, Air, & Soil Pollution*, 227, 1-16, 2016.

841 Hersbach, H., Bell, B., Berrisford, P., Hirahara, S., Horányi, A., Muñoz-Sabater, J., Nicolas,  
842 J., Peubey, C., Radu, R., Schepers, D., Simmons, A., Soci, C., Abdalla, S., Abellan, X.,  
843 Balsamo, G., Bechtold, P., Biavati, G., Bidlot, J., Bonavita, M., Chiara, G., Dahlgren, P.,  
844 Dee, D., Diamantakis, M., Dragani, R., Flemming, J., Forbes, R., Fuentes, M., Geer, A.,  
845 Haimberger, L., Healy, S., Hogan, R. J., Hólm, E., Janisková, M., Keeley, S., Laloyaux,  
846 P., Lopez, P., Lupu, C., Radnoti, G., Rosnay, P., Rozum, I., Vamborg, F., Villaume, S.,

847 and Thépaut, J. N.: The ERA5 global reanalysis, *Quarterly Journal of the Royal*  
848 *Meteorological Society*, 146, 1999-2049, 10.1002/qj.3803, 2020.

849 Hong, C., Zhang, Q., Zhang, Y., Davis, S. J., Tong, D., Zheng, Y., Liu, Z., Guan, D., He, K.,  
850 and Schellnhuber, H. J.: Impacts of climate change on future air quality and human health  
851 in China, *Proceedings of the National Academy of Sciences*, 116, 17193-17200, 2019.

852 Hou, P., and Wu, S.: Long-term changes in extreme air pollution meteorology and the  
853 implications for air quality, *Scientific reports*, 6, 1-9, 2016.

854 Jia, B., Wang, Y., Yao, Y., and Xie, Y.: A new indicator on the impact of large-scale circulation  
855 on wintertime particulate matter pollution over China, *Atmospheric Chemistry and*  
856 *Physics*, 15, 11919-11929, 2015.

857 Kan, H., London, S. J., Chen, G., Zhang, Y., Song, G., Zhao, N., Jiang, L., and Chen, B.:  
858 Differentiating the effects of fine and coarse particles on daily mortality in Shanghai,  
859 China, *Environment international*, 33, 376-384, 2007.

860 Kan, H., Chen, R., and Tong, S.: Ambient air pollution, climate change, and population health  
861 in China, *Environment international*, 42, 10-19, 2012.

862 Kay, J. E., Deser, C., Phillips, A., Mai, A., Hannay, C., Strand, G., Arblaster, J. M., Bates, S.,  
863 Danabasoglu, G., and Edwards, J.: The Community Earth System Model (CESM) large  
864 ensemble project: A community resource for studying climate change in the presence of  
865 internal climate variability, *Bulletin of the American Meteorological Society*, 96, 1333-  
866 1349, 2015.

867 Knutti, R., Furrer, R., Tebaldi, C., Cermak, J., and Meehl, G. A.: Challenges in combining  
868 projections from multiple climate models, *Journal of Climate*, 23, 2739-2758, 2010.

869 Kong, L., Tang, X., Zhu, J., Wang, Z., Li, J., Wu, H., Wu, Q., Chen, H., Zhu, L., and Wang,  
870 W.: A 6-year-long (2013–2018) high-resolution air quality reanalysis dataset in China



871 based on the assimilation of surface observations from CNEMC, Earth System Science  
872 Data, 13, 529-570, 2021.

873 Li, K., Liao, H., Cai, W., and Yang, Y.: Attribution of Anthropogenic Influence on  
874 Atmospheric Patterns Conducive to Recent Most Severe Haze Over Eastern China,  
875 Geophysical Research Letters, 45, 2072-2081, 10.1002/2017gl076570, 2018.

876 Li, Q., Zhang, R., and Wang, Y.: Interannual variation of the wintertime fog–haze days across  
877 central and eastern China and its relation with East Asian winter monsoon, International  
878 Journal of Climatology, 36, 346-354, 2016.

879 Liu, C., Zhang, F., Miao, L., Lei, Y., and Yang, Q.: Future haze events in Beijing, China: When  
880 climate warms by 1.5 and 2.0°C, International Journal of Climatology, 40, 3689-3700,  
881 10.1002/joc.6421, 2019.

882 Liu, Q., Jia, X., Quan, J., Li, J., Li, X., Wu, Y., Chen, D., Wang, Z., and Liu, Y.: New positive  
883 feedback mechanism between boundary layer meteorology and secondary aerosol  
884 formation during severe haze events, Scientific reports, 8, 1-8, 2018.

885 Liu, T., Gong, S., He, J., Yu, M., Wang, Q., Li, H., Liu, W., Zhang, J., Li, L., Wang, X., Li, S.,  
886 Lu, Y., Du, H., Wang, Y., Zhou, C., Liu, H., and Zhao, Q.: Attributions of meteorological  
887 and emission factors to the 2015 winter severe haze pollution episodes in China's Jing-  
888 Jin-Ji area, Atmospheric Chemistry and Physics, 17, 2971-2980, 10.5194/acp-17-2971-  
889 2017, 2017.

890 Pei, L., Yan, Z., Sun, Z., Miao, S., and Yao, Y.: Increasing persistent haze in Beijing: potential  
891 impacts of weakening East Asian winter monsoons associated with northwestern Pacific  
892 sea surface temperature trends, Atmospheric Chemistry and Physics, 18, 3173-3183,  
893 2018.

894 Pendergrass, D., Shen, L., Jacob, D., and Mickley, L.: Predicting the impact of climate change  
895 on severe wintertime particulate pollution events in Beijing using extreme value theory,  
896 *Geophysical Research Letters*, 46, 1824-1830, 2019.

897 Petäjä, T., Järvi, L., Kerminen, V.-M., Ding, A., Sun, J., Nie, W., Kujansuu, J., Virkkula, A.,  
898 Yang, X., and Fu, C.: Enhanced air pollution via aerosol-boundary layer feedback in  
899 China, *Scientific reports*, 6, 1-6, 2016.

900 Qiu, L., Yue, X., Hua, W., and Lei, Y.-D.: Projection of weather potential for winter haze  
901 episodes in Beijing by 1.5 °C and 2.0 °C global warming, *Advances in Climate Change*  
902 *Research*, 11, 218-226, 10.1016/j.accre.2020.09.002, 2020.

903 Renhe, Z., Li, Q., and Zhang, R.: Meteorological conditions for the persistent severe fog and  
904 haze event over eastern China in January 2013, *Science China Earth Sciences*, 57, 26-35,  
905 2014.

906 Sexton, D. M., McSweeney, C. F., Rostron, J. W., Yamazaki, K., Booth, B. B., Murphy, J. M.,  
907 Regayre, L., Johnson, J. S., and Karmalkar, A. V.: A perturbed parameter ensemble of  
908 HadGEM3-GC3. 05 coupled model projections: part 1: selecting the parameter  
909 combinations, *Climate Dynamics*, 56, 3395-3436, 2021.

910 Shen, L., Jacob, D. J., Mickley, L. J., Wang, Y., and Zhang, Q.: Insignificant effect of climate  
911 change on winter haze pollution in Beijing, *Atmospheric Chemistry and Physics*, 18,  
912 17489-17496, 10.5194/acp-18-17489-2018, 2018.

913 Sun, Y., Jiang, Q., Wang, Z., Fu, P., Li, J., Yang, T., and Yin, Y.: Investigation of the sources  
914 and evolution processes of severe haze pollution in Beijing in January 2013, *Journal of*  
915 *Geophysical Research: Atmospheres*, 119, 4380-4398, 2014.

916 Tie, X., Huang, R.-J., Cao, J., Zhang, Q., Cheng, Y., Su, H., Chang, D., Pöschl, U., Hoffmann,  
917 T., and Dusek, U.: Severe pollution in China amplified by atmospheric moisture,  
918 *Scientific Reports*, 7, 1-8, 2017.

919 Wang, J.-L., Zhang, Y.-h., Shao, M., Liu, X.-l., Zeng, L.-m., Cheng, C.-l., and Xu, X.-f.:  
920 Quantitative relationship between visibility and mass concentration of PM<sub>2.5</sub> in Beijing,  
921 Journal of environmental sciences, 18, 475-481, 2006.

922 Wang, L., Wei, Z., Yang, J., Zhang, Y., Zhang, F., Su, J., Meng, C., and Zhang, Q.: The 2013  
923 severe haze over southern Hebei, China: model evaluation, source apportionment, and  
924 policy implications, Atmospheric Chemistry and Physics, 14, 3151-3173, 2014a.

925 Wang, Y., Yao, L., Wang, L., Liu, Z., Ji, D., Tang, G., Zhang, J., Sun, Y., Hu, B., and Xin, J.:  
926 Mechanism for the formation of the January 2013 heavy haze pollution episode over  
927 central and eastern China, Science China Earth Sciences, 57, 14-25, 2014b.

928 Xu, M., Chang, C. P., Fu, C., Qi, Y., Robock, A., Robinson, D., and Zhang, H. m.: Steady  
929 decline of east Asian monsoon winds, 1969–2000: Evidence from direct ground  
930 measurements of wind speed, Journal of Geophysical Research: Atmospheres, 111, 2006.

931 Xu, P., Chen, Y., and Ye, X.: Haze, air pollution, and health in China, Lancet, 382, 2067,  
932 10.1016/S0140-6736(13)62693-8, 2013.

933 Yamazaki, K., Sexton, D. M., Rostron, J. W., McSweeney, C. F., Murphy, J. M., and Harris,  
934 G. R.: A perturbed parameter ensemble of HadGEM3-GC3. 05 coupled model  
935 projections: part 2: global performance and future changes, Climate Dynamics, 56, 3437-  
936 3471, 2021.

937 Yin, Z., and Wang, H.: Role of atmospheric circulations in haze pollution in December 2016,  
938 Atmospheric Chemistry and Physics, 17, 11673-11681, 10.5194/acp-17-11673-2017,  
939 2017.

940 Zhang, Q., Ma, Q., Zhao, B., Liu, X., Wang, Y., Jia, B., and Zhang, X.: Winter haze over North  
941 China Plain from 2009 to 2016: Influence of emission and meteorology, Environ Pollut,  
942 242, 1308-1318, 10.1016/j.envpol.2018.08.019, 2018.

943 Zhang, R., Jing, J., Tao, J., Hsu, S.-C., Wang, G., Cao, J., Lee, C. S. L., Zhu, L., Chen, Z., and  
944 Zhao, Y.: Chemical characterization and source apportionment of PM 2.5 in Beijing:  
945 seasonal perspective, *Atmospheric Chemistry and Physics*, 13, 7053-7074, 2013.

946 Zhang, L., Wilcox, L. J., Dunstone, N. J., Paynter, D. J., Hu, S., Bollasina, M., ... & Zou, L.  
947 (2021). Future changes in Beijing haze events under different anthropogenic aerosol  
948 emission scenarios. *Atmospheric Chemistry and Physics*, 21(10), 7499-7514.

949 Zhang, Z., Gong, D., Mao, R., Kim, S. J., Xu, J., Zhao, X., and Ma, Z.: Cause and predictability  
950 for the severe haze pollution in downtown Beijing in November-December 2015, *Sci*  
951 *Total Environ*, 592, 627-638, 10.1016/j.scitotenv.2017.03.009, 2017.

952

953